ABSTRACT

Title of Thesis:	DEVELOPING AN IN SITU SPRAYABLE BIOSCAFFOLD WITH ANTIMICROBIAL PROPERTIES AS AN EMERGENCY BURN WOUND DRESSING
	Joseph Hunter, Master of Science, 2018
Thesis directed by:	Professor Peter Kofinas, Department of Chemical and Biomolecular Engineering

Commercially available silver dressings and their associated application/removal protocols suffer from several serious drawbacks, including: inability to monitor the burn wound beneath the opaque dressing, high costs, traumatic debridement due to a non-degradable mesh, delays involved with transporting a patient to a location where sterile conditions can be maintained, and restrictions upon when a silver dressing can be used. The results of this work present a promising proof of concept for an *in situ* sprayable synthetic polymer containing a silver salt that was found to allow for wound observation (transitions to clear at body temperature), degrade in a biocompatible manner, release broad-spectrum antimicrobial silver in a controlled manner, and can be safely applied in the acute period following a burn in the absence of sterile conditions with little detriment to wound healing *in vivo* and less than 20% reduced viability *in vitro*.

DEVELOPING AN IN-SITU SPRAYABLE BIOSCAFFOLD WITH ANTIMICROBIAL PROPERTIES AS AN EMERGENCY BURN WOUND DRESSING

by

Joseph Hunter

Thesis submitted to the Faculty of the Graduate School of the
University of Maryland, College Park, in partial fulfillment
of the requirements for the degree of
Master of Science,
2018

Advisory Committee:
Professor Peter Kofinas, Chair
Professor Giuliano Scarcelli
Professor Gregg Duncan

Acknowledgements

I would like to thank Peter and John for their support that can only be described as above and beyond what can be expected from their respective positions, and I owe much of the success of this study to their help and guidance. I would like to thank my committee members, the members of the Kofinas, Lloyd, and Briber labs, and LK and Dr. Sandler from Children's National Hospital for your insight, experience, and advice. I would also like to thank Caroline for her everlasting support.

Table of Contents

List of Figures

Fig 2.9: MTT assay performed on ETAC (Ag) PLGA-PEG samples blowspun onto glass slides. All fluorescence readings are normalized against control/media sample which contained only cells and media. Horizontal bar indicates target acceptable cytotoxicity.

Chapter 1: Background and Motivation

1.1 Significance

Burn wound infections are one of the most important and potentially serious complications that occur in the acute period following injury and they are the leading cause of mortality in burn victims: 75% of victims with burns that cover greater than 40% Total Body Surface Area (TBSA) die from infection, and most burn-related deaths (54%) are due to septic shock[1]. Sepsis is a life-threatening complication characterized by organ failure, and a mortality rate of roughly 30%-40%[2]. This high mortality can be largely attributed to the rapid progression of sepsis to more severe conditions, such as septic shock[2–7]. Current clinical methods utilized to determine the presence and identity of sepsis-inducing agents (SIAs) can take more than two days to provide relevant diagnostic information, and complications and mortality occur on time scales much shorter than this, even from the start of intensive care: Within hours of suspecting sepsis, broad spectrum antibiotics are administered, long before the blood culture results are obtained. Use of broad spectrum antibiotics before determining the SIA's identity (and thereby, its sensitivity to antibiotics) results in improper or ineffective use of antibiotics and can worsen the patient's condition and merely improve the antibiotic resistance of the infection[3,8–11]. Furthermore, delayed or inappropriate antibiotic treatment has been found to raise sepsis mortality by a factor between 1.6x and 5x, depending on the population stratification used[3]. The state of the current antibiotic-resistant infection crisis has resulted in a strong demand for a rapid, broad-spectrum treatment method that can be utilized as early as possible from the suspected onset of

infection. Additionally, fewer antibiotics are being approved as microbes only develop more resistances, which is creating an urgent demand for alternative methods of treating infection[9].

Silver has emerged as an effective universal antimicrobial agent through its oligodynamic effect and has been found to have low minimum inhibitory concentrations (MICs) and minimum bacteriocidal concentrations (MBCs) for Gram negative, Gram positive, and fungal infections with low risk of resistance development[12–16]. Silver can also be coupled with antibiotic treatment to dramatically potentiate the antimicrobial effect of its partner: antibiotics coupled with sublethal concentrations of silver were found to kill up to 1000-fold more bacteria than the antibiotic alone[14,17]. These properties make silver an attractive solution to treating burn-related infections, and though its clinical use has been relatively underutilized due to cytotoxicity concerns, current applications exist such as wound dressings that utilize a passive, controlled release of silver[18]. The significance of this work is that it provides a proof of concept for a silver-based dressing that would provide a crucial first step in addressing these preventable, fatal burn wound infections. This study would be beneficial both on a practical basis to first responders as a catch-all answer to potential infection that does not compromise subsequent treatment efforts, and on a clinical policy basis in that it presents a compelling argument for the use of silver as an antimicrobial agent earlier in infection treatment, and more often in infection response efforts.

1.2 Innovation

Though silver dressings are effective in their antimicrobial activity, they suffer from several application-based drawbacks: (i) Non-degradable dressings applied directly to a re-epithelializing wound bed can become "stuck" (intertwined with new tissue deposition and proliferating cells) and require debridement. Removing the dressing at this stage not only slows the healing process, but also increases the risk of infection[19,20]. (ii) As with most gauze-based treatments, silver dressings are opaque, and the wound bed cannot be observed while the dressing is applied. Thus, the state of the burn wound will be unknown for the duration of silver treatment, preventing those providing treatment from explicitly knowing if the wound is worsening, or when the dressing should be removed. During the dynamic, acute period following burn wound infliction, the burn wound must be observed—which results in the necessary, complete removal of any opaque dressing or sulfadiazine cream applied by first responders before wound observation or treatment can take place[32]. (iii) Silver salts are loaded into expensive, inelastic, non-patient-specific gauze or meshes. This results in wasted material and inefficient application. (iv) The protocol required to apply a silver dressing is not possible in the acute period immediately after a serious burn: wound dressings are applied under aseptic conditions and technique, and often require access to running water and electricity (for handwashing steps or sterile assurance otherwise)[21]. This restricts the locations in which a silver dressing can be safely applied to a laboratory or a hospital with the necessary equipment. Thus, it appears that the silver dressings are beneficial largely because they contain silver, and nearly all drawbacks are due to the silver being restricted to a gauze application medium.

Innovation from this stage would involve capitalizing upon the use of silver in early infection treatment and applying it to the wound bed through a method that does not require sterile technique or possess the drawbacks of gauze dressings.

Solution blow spinning (SBS) is a nanofiber deposition alternative to electrospinning that does not require expensive equipment or an electrically conductive site of deposition[22]. SBS involves a volatile solution containing polymer which can be sprayed through a simple CO_2 airbrush onto any surface, coating it with polymer nanofibers as the volatile solvent disperses[22]. This is an improvement upon electrospinning, which produces stiff and relatively brittle meshes of PLGA and requires the nanofiber mats to be assembled on a conductive surface and then transferred to the site of deposition later. Poly(lactic-co-glycolic acid) and polyethylene glycol blends (PLGA-PEG) deposited via SBS results in a mesh with desirable delivery properties: (i) The ratio of lactide groups to glycolide groups in the PLGA controls the tensile modulus of the resulting blowspun fiber mat, allowing for PLGA to be optimized to have comparable mechanical properties to the surface it is being deposited onto[22]. (ii) PLGA-PEG meshes have also been found to have adjustable degradation rates and do not negatively influence the viability of cells growing nearby[23]. (iii) Due to the thermal properties of PEG, which forms crystalline domains during the blowspinning process, PLGA-PEG possesses a PEG-concentration-dependent melting transition at approximately 31°C, the same as PEG. This transition causes PLGA-PEG meshes to transition to a more adherent, elastic, transparent film around typical human body temperature, 37 °C [23]. (iv) By using a

hand-held, CO_2 powered airbrush, the PLGA-PEG mesh is *in situ* deliverable independent of access to electricity, running water, or sterile conditions: This method is expected to be semi-sterile, due to the sterilizing nature of the volatile blowspinning solvents acetone and ethyl acetate, and the non-contact nature of the application: nothing comes into direct or indirect contact with the immune-compromised skin except for the silver-containing polymer—the active antimicrobial agent and CO_2. Procedure for dressing wounds require that anything that directly or indirectly come into contact with the wound (all tools, gloves, dressings, etc) to be sterile and that aseptic technique is observed for the entirety of treatment. This typically is only possible in a controlled lab or hospital environment. I propose that for SBS-delivered silver dressings, neither the operator's hands, the operating environment, nor the blowspinning solution need to be sterilized ahead of time, and the airbrush itself can be quickly sterilized with an ethanol rinse prior to use, allowing for on-site application by first responders.

I hypothesized that incorporating a silver salt that dissolves in volatile solvent into a PLGA-PEG blowspinning solution will result in an *in situ* sprayable antimicrobial mesh that can be used in both emergency and non-emergency situations by first responders to a serious burn wound under suspicion of potential infection. Using blowspun PLGA-PEG as a silver delivery material presents several innovative advantages that counter the drawbacks of silver dressings: (i) (Ag) PLGA-PEG is expected to be biodegradable/erodible in roughly 4 weeks, obviating the need for debridement, (ii) (Ag)PLGA-PEG is expected to be opaque while being blowspun so wound bed coverage can be assured, and will transition into a transparent mesh after

adjusting to body temperature, allowing for the wound bed to be monitored closely during the healing process and during the dynamic, acute period following burn wound infliction, during which the wound must be observed for changes. (iii) (Ag) PLGA-PEG is expected to be capable of being applied to burn wound victims on-scene or in-transit without the need for electricity, running water, or sterile conditions because of its non-contact, innately semi-sterile nature, (iv) (Ag) PLGA-PEG can be applied directly *in situ* in a wound-specific manner, providing efficient coverage of the wound area while minimizing waste of the already inexpensive polymer material.

1.3 Background

1.3.1 Silver

1.3.1.1 Broad spectrum antimicrobial activity

Silver salt (AgX) was chosen as the model antimicrobial agent due to its desirable properties as a long-term solution to the current microbial drug-resistance crisis. Silver has been found to be broad-spectrum, rapid-acting, antibiotic-potentiating, resensitization-inducing, and possesses a oligodynamic activity mechanism, which is generally described as the tendency of heavy metals to elicit biocidal properties. The biocidal activity of silver specifically has been found to have a low risk of silver resistance development[16].

(Kim et al., Nanomedicine, 2007) Describes the broad-spectrum nature of silver particles in inhibiting Gram positive, Gram negative, and fungal microbial growth in a

agar surface scenario. Therein, a typical disc diffusion method quantified the difference in microbial density between the region of the plate containing silver particles released from diffusive discs and unaffected regions far from the disc. Minimum Inhibitory Concentration (MIC), or the least amount of silver required to prevent micribal growth, is determined here by the lowest concentration of silver particles required to yield a growth inhibition ratio within a statistically insignifcant range from the positive control. In each case, the effective AgNP concentration required to achieve MIC is on a fairly comparable nanomolar scale, generally indicating similar inhibitory effectiveness against a wide breadth of microbes. These findings are consistent with previous studies on Ag salts and purported microbe inhibition mechanisms:Ag salts and AgNPs have been observed to have comparable MICs[12]. The true mechanism of silver activity is currently being investigated, though findings currently suggest that a major component of its antimicrobial effect is the nature of Ag+ to bind to (and thereby render disfunctional) negatively charged microbial cellular components such as the cell membrane, mitochondrial enzymes, and genetic material[24,25]. Permeabilizing microbial membranes, preventing respiration, and interfering with genetic replication are feasibly broad-spectrum effective bacteriocidal/growth inhibition mechanisms.

1.3.1.2 Effectiveness against antibiotic-resistant microbes

(Lara, World Journal of Microbiology and Biotechnology, 2009) follows a broth microdilution analysis and a subsequent luciferase assay in order to evaluate the susceptibility of mutlidrug-resistant bacterial strains to silver particles by quantifying

Minimum Inhibitory Concentration (MIC) and Minimum Bacteriocidal Concentration (MBC). Microdilution methods of MIC/MBC determination tend to be more relevant to instances where silver and its source are submerged entirely, such as with silver-coated device implants, though the relative values obtained in this study are worth noting: No significant difference was detected between the MIC, MBC, and MIC/MBC ratio (secondary measure of bacteriocidal effectiveness) of drug-resistant bacteria and drug-susceptible bacteria, indicating that silver particles are equally effective against either. Additionally, silver resistance has been described as unstable, uninheritable, and mostly relative, which presents a low-resistance-risk antimicribal agent that is effective against a broad spectrum of drug-resistant microbes[16].

1.3.1.3 Resensitization and repotentiation

Resensitization and potentiation refer to the mechanism in which silver can obviate or otherwise reduce antimicrobial resistance of a microbial strain or compound the efficacy of an antibiotic. A study by Morones-Ramirez *et al* in Science Translational Medicine demonstrated both effects against Gram-negative *E. coli*[17]. In this study, it is demonstrated that administering sublethal concentrations of silver can dramatically compound the antimicrobial effects of an antibiotic against a resistant microbe with increasing concentrations of silver. This effect is conserved across several different antibiotics, and administration of Tetracycline in conjunction with Ag+ reduces the antibiotic resistance of Tetracycline-resistant strains to an insignificant difference from its vulnerable wildtype phenotype[17].

1.3.1.4 Silver dressings

Currently commercially available silver wound dressings generally involve affixing silver to a fibrous base: Silver in these dressings exist in several possible states: (i) Elemental (Ag+, AgNPs) (ii) Inorganic compounds (Silver salts, AgX, etc) (iii) Organic complexes (silver alginate, silver-apatite complexes, etc)[26]. These various states can also exist in the silver dressing in various locations including: (i) physical coating (ii) chemical association with fibers (iii) physical impregnation[26]. The silver states, locations, and concentrations used can be highly variable between different products, though the intended mechanism of activity is conserved: silver is introduced into the wound bed through diffusion, at which point antimicrobial Ag^+ ions are donated from their source compound and released into the local area, generally due to the tendency of silver compounds to ionize in aqueous solutions.

In most cases, silver dressings are not administered until there is substantial evidence of localized infection long after infection has taken hold[26]. This is largely due to controversial claims on the risks of clinical use of silver: There are claims that silver categorically can delay re-epithelialization and cause local and systemic toxicity, though this notion has been largely countered by the preponderance of evidence that demonstrate that appropriate use of silver dressings (i.e., while there is infection or suspicion thereof) can accelerate treatment and improve antibiotic efforts[13,26–29]. Additionally, there are proponents of utilizing silver dressings on all immune-compromised burns for the first 48 hours of treatment, during which the dynamic nature of the burn wound appearance must be monitorable[26]. Typically, there is a thorough

examination of the patient, the wound, and any preexisting or special circumstances that would influence the decision of whether to use a silver dressing in place of an inert dressing, though exception is given to situations in which there is a high likelihood that an infection has taken place (covert or early stages), especially because silver salt antimicrobial activity is most effective before microbial colonization has taken place[26]. As such, quick response to a suspected burn wound infection is hampered largely by the time it takes to physically transport a patient to a sterile treatment location, which can be extensive in rural locations, and by the time it takes to identify the microbe responsible.

1.3.2 PLGA-PEG

The advantage to utilizing silver dressings is that they are effective antimicrobial dressings due to their silver content, though performance suffers from the mechanical drawbacks of restricting silver release to gauze pads through a sterile-contact application method. To innovate upon the current clinically standard silver dressing, a new treatment should: (i) Contain and controllably release silver in its ionic form (Ag^+) or in potent particle form (AgNP) (ii) Obviate the need for debridement (iii) Allow the burn wound injury to be observed during the healing process, especially during the first 48 hour acute period immediately after the burn wound injury has been sustained (iv) Not require sterile application environments (e.g., non-contact methods, sprayable deposition) or otherwise delay treatment past the acute period immediately after a severe burn wound has been sustained.

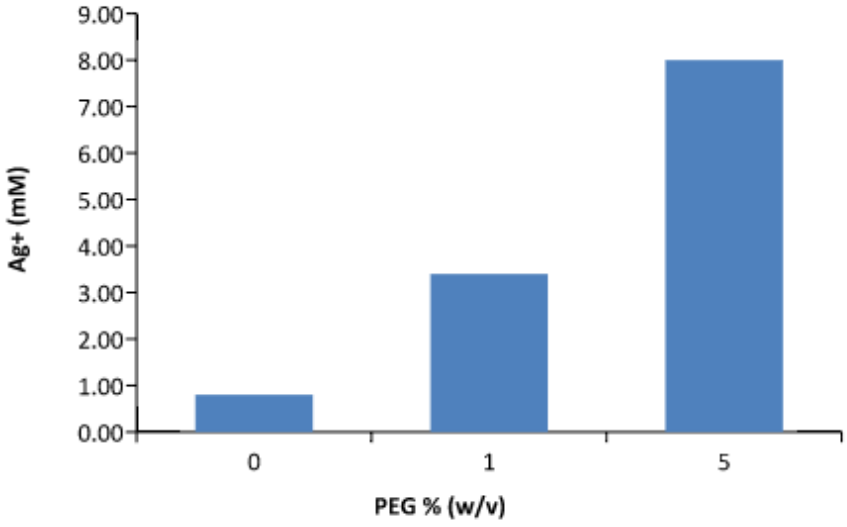

Fig1.1: Preliminary data describing the correlation between the PEG (weight/volume)% and the amount of Ag+(mM) released from a submerged (Ag) PLGA-PEG mesh detected by Mohr Titration in 24hr.

Solution blowspinning is a portable, cost-efficient nanofiber deposition method that involves passing a volatile solvent containing concentrated polymer through a simple CO_2 airbrush, resulting in a conformal *in situ* fiber mat[22,23]. Preliminary studies performed by the Functional Materials Laboratory (University of Maryland, College Park) suggested that silver salts such as silver nitrate can be incorporated into blowspinning solutions containing poly(lactic-co-glycolic acid) (PLGA) and released at a rate proportional to the amount of polyethylene glycol (PEG) present. PLGA-PEG meshes experience a melting transition at approximately 31° C, producing several structural changes that (i) transforms the fiber mesh into a conformal film of rubbery polymer (ii) results in the permanent loss of fiber morphology (iii) causes the polymer melt to transition from white in appearance to transparent[22,23]. These properties in a

clinical context have innovative applications: PLGA-PEG meshes can be solution blowspun safely *in situ* topically or internally in a manner that allows the polymer mesh to be opaque as it is being blowspun (so the operator can easily see wound coverage progress) but will transition to clear as the polymer approaches 37°*C*, conveniently near body temperature. Once the polymer film becomes clear in a matter of minutes, the underlying wound can be visualized for progression of healing or infection.

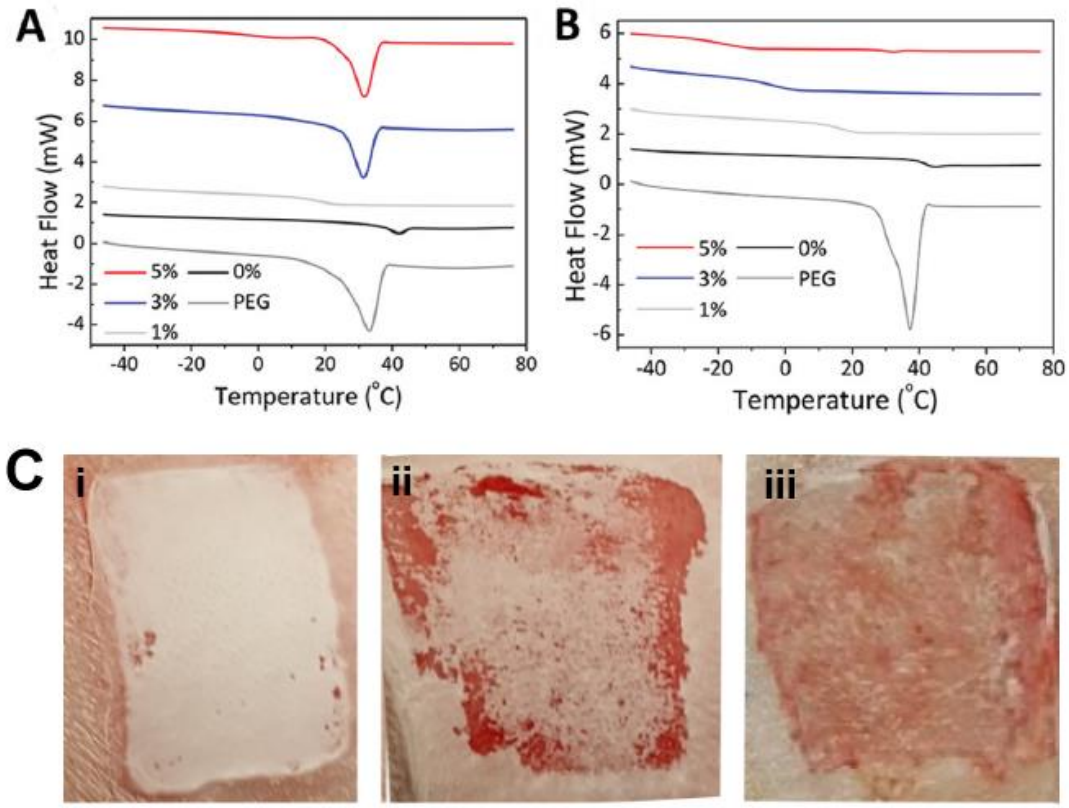

Fig1.2 (A) The first heating cycle of PLGA-PEG at varying concentrations of PEG compared to the original melting transition of PEG. Values are Y-shifted for readability. (B) The second heating cycle of PLGA-PEG at varying concentrations of PEG compared to the original melting transition of PEG. Values are Y-shifted for readability[23]. (C) Images of on-wound PLGA-PEG (i) freshly blowun, before transitioning (ii) transitioning (iii) completely transitioned.

Fig 1.4 demonstrates the melting transition of PLGA-PEG polymers as a function of PEG content and heating iteration through Differential Scanning Calorimetry (DSC).

Fig 1.4A shows a Y-shifted overlay of various PLGA-PEG copolymer blend heat cycles: the PEG melting point transition peak at approximately 37°C is most prominent at higher concentrations of PEG within the blowspun film. Fig 1.4B is the second heating cycle of the same samples: all melting transitions are absent because the PEG does not recrystallize after the PLGA-PEG blend homogenizes. Fig 1.4C are images of untransitioned PLGA-PEG (left), transitioning PLGA-PEG (middle), and transitioning PLGA-PEG (right) during the porcine wound healing study discussed in (Section TBA).

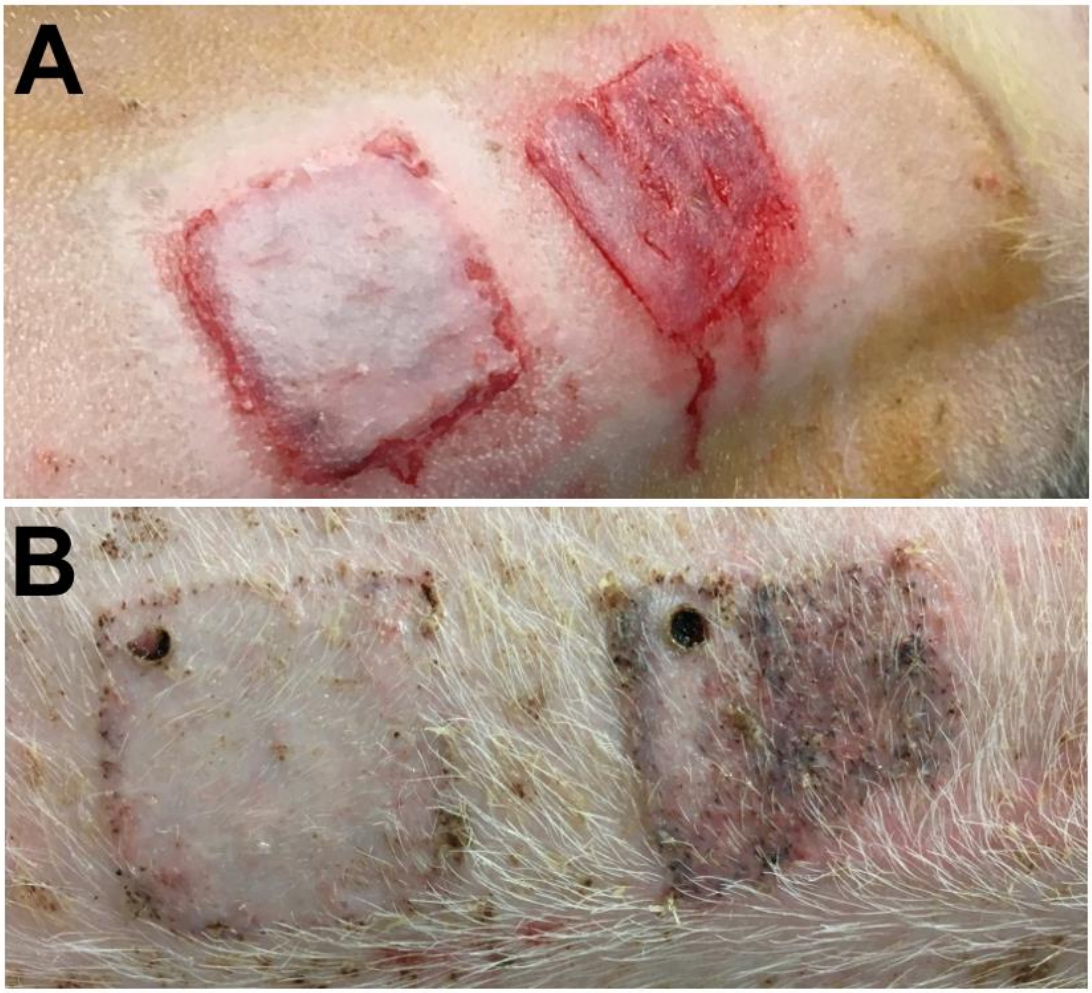

Fig. 1.3: A porcine dorsal dermal wound healing study (A) Immediately after wound coverage of the left injury (B) One month from wound coverage. Dark circles are where biopsy samples were collected.

A previous porcine wound healing study by the Functional Materials Laboratory (UMCP) compared healing progression between an uncovered wound (Right, Figure 1.5A) and a wound treated with blowspun PLGA-PEG shortly after the wound was simulated (Left, Figure 1.5A). A month later, total wound area measurements and qualitative evaluation by a surgeon demonstrated that PLGA-PEG coverage alone enhances wound recovery. This is hypothesized to be due to the biocompatibility and biodegradabilty of PLGA, the porous nature of PLGA-PEG meshes allowing oxygen

diffusion into the wound bed, and simple physical protection of the wound from its environment.

Chapter 2: Development and evaluation of ETAC (Ag) PLGA-PEG antimicrobial nanofiber mat

2.1 Methods

2.1.1 Solution Blowspinning

A commercially available airbrush (Master Airbrush G22-SET, 0.2 mm nozzle diameter) was used in all SBS protocols involved in the following experiments. For porcine *in vivo* wound healing studies, a handheld, CO_2 canister-fed regulator rig was used, and in all other studies gas was supplied through a CO_2 tank equipped with a regulator. The distance between the airbrush nozzle and the application surface was approximately 10 cm for all studies.

2.1.2 Scanning Electron Microscopy/Energy Dispersive X-ray Spectroscopy

A Hitachi SU-70 Schottky field emission gun scanning electron microscope was used to image gold sputter coated ETAC (Ag) PLGA-PEG nanofiber mats. The sample types compared include ETAC (0 mg/mL–9.9 mg/mL silver nitrate) PLGA-PEG and acetone (0mg/mL-9.9mg/mL silver nitrate) PLGA-PEG. Several snapshots (N=3-5) were taken across the surface of the fiber mat through SEM-EDS and measured for carbon/oxygen-normalized silver wt% based on relative abundance. Carbon and oxygen are the non-

hydrogen atoms that exclusively make up both PLGA and PEG, so EDS-determined abundance of each element was weighted by their std. weight before normalizing silver wt% against the detected wt% of carbon and oxygen.

2.1.3 Accumulation/Release Rate of Silver

To approximate an aqueous wound bed, 1mL nanofiber mats (acetone (9.9mg/mL silver nitrate) PLGA-PEG) were blowspun onto a glass slide and submerged in 5mL of water and maintained at a body temperature oven (37°C) for a month. Intermittently at regular intervals (See Fig. 2.3 for timepoints), a small volume was collected and Mohr titrated for the presence of silver to crudely approximate the amount of silver that would be released *in vivo*. The amount recorded at each time point was then converted to a μmol concentration based on the volume of the well, and water was replenished. Both *Accumulation* and *Release Rate* of Ag were tracked: *Accumulation* is the sum of the Ag released at each time point, which tracks the amount of silver released as it accumulates in solution. *Release Rate* is the derivative of this curve. After implantation, eluted silver is constantly being exchanged with the wound exudate and does not accumulate at the wound site. *Release Rate* more accurately represents the amount of silver that the wound will be experiencing at any instant in time.

Accumulation and *Release Rate* were plotted and compared to estimates of the Minimum Inhibitory Concentrations (MICs: the least amount of silver needed to inhibit

growth of microbes in solution) and Minimum Bactericidal Concentrations (MBCs: the least amount of silver needed to kill all microbes in solution) obtained by approximating the dry mass equivalent of each concentration in the volume present at each timepoint. Additionally, a similar test was performed to gain insight into any potentially confounding factors: Three parameters that were expected to influence the amount of silver present or the amount of silver released included the solvent used (EtAc or Ac), the volume of blowspinning solution (0.5mL-1mL), and the concentration of silver nitrate in the original blowspinning solution(0.5mg/mL-5mg/mL Ag).

2.1.4 Differential Scanning Calorimetry

1mL ETAC (0.5mg/mL-5mg/mL Ag) PLGA-PEG was blowspun onto glass slides and cut with a razor blade to 7-13mg in weight and sealed in an aluminum hermetic pan. Differential Scanning Calorimetry (DSC) was performed in a 2-cycle heating ramp at 20C/min from -50C to 80C.

2.1.5 Dynamic Mechanical Analysis

1mL ETAC PLGA-PEG and 1mL ETAC (5mg/mL Ag) PLGA-PEG was blowspun onto glass slides and cut with a razor blade to approximately 15mm x 5mm. Ends are taped to avoid clamping damage. Dynamic Mechanical Analysis (DMA) force ramp was used to obtain the Young's Modulus of typical ETAC (Ag) PLGA-PEG nanofiber mat and to compare these measurements against ETAC (Ag) PLGA-PEG mats properties. Young's modulus recorded from elastic region at 0-5% strain.

2.1.6 Kirby-Bauer Disc Diffusion for Antimicrobial Activity

As is conventional with an interfacial antimicrobial activity test, a modified Kirby-Bauer Disc Diffusion test was used to compare the antimicrobial activity of a blowspun ETAC (Ag) PLGA-PEG to 10ug Gentamicin: Mueller Hinton agar was cultured with *S.aureus* and *E.coli* cultured in LB broth to 0.08-0.12 at 635nm with photometer, producing 1-2x10^8 CFU/mL, inoculated at 100uL into MB agar. ZOI measurements recorded after 24 hours at 37°C. Both treatments were tested against Gram-positive (*S. aureus*) and Gram-negative (*E. coli*) strains. Positive control made by loading 10ug gentamicin into sterile KB disc. To create the EA (Ag) PLGA-PEG "discs," 1mL of 5mg/mL (Ag-High), 1mg/mL (Ag-Med), 0.5mg/mL (Ag-Low), or 0mg/mL (PLGA) silver in EA PLGA-PEG blowspinning solution was aseptically blowspun directly onto a small 10mm sterile gauze disc.

2.1.7 MTT Cytotoxicity Assay

An MTT Absorbance assay was used to compare cell viability between nanofiber mats containing various clinically relevant concentrations of silver. Murine fibroblast L929 cells were cultured for 24 hours in minimum essential medium culture supplemented with 100IU/mL penicillin, 100ug/mL streptomycin, 4mM glutamine, and 10% fetal bovine serum. Cells were loaded into 96-well plate at 1x10^4 per well. Glass slides were coated with 1mL of silver-containing ETAC PLGA-PEG blowspinning solution (0.09-4.95 Ag mg/mL) (which eluted to ~16ug/mL concentration in media solution at 24 hours). These samples were incubated with 10mL MEM to generate stock solution which is diluted 1x-100x with additional MEM. Cell culture was aspirated and replaced with 100uL of each respective sample, incubated for 24 hours, and a WST1

survival assay is performed. Absorbance readings were normalized and relative to the control.

2.1.8 Porcine *in vivo* Wound Healing

Several *in vivo* porcine wound healing experiments were run in which anesthetized Yorkshire piglets were given up to 8 simulated dorsal burn wounds 1500mm^2 in size with a Dermatome tool at 0.4mm-0.6mm cut thickness. The wounds were immediately coated with 1mL EtAc (0-5mg/mL Ag) PLGA-PEG, ETAC PLGA-PEG, Tegaderm, or were left uncovered. Blowspinning was performed with a modified handheld CO_2 canister-powered commercial airbrush. The piglets were returned to their cages and allowed to wake up, and wounds were then monitored over the span of a month, with dermal biopsies and photographs collected every other week. Biopsies were collected after anesthetization from the center and the ends of the burn wound. Healing was evaluated by biweekly wound size measurements, appearance of the wound, and through biopsy analysis. To track the fate of PLGA-PEG, a formula was developed in which fluorescein end-capped PLGA (PLGA-f) replaced a fraction of the PLGA in PLGA-PEG blowspinning solution (25:75, PLGA-f:PLGA). which produces a similar nanofiber mat detectable with fluorescence microscopy. These nanofiber mats were deposited onto a wound bed in a replicate porcine healing study, and biopsy samples were taken approximately 2 weeks from initial wound coverage, after scab formation. A cross section of the biopsy was performed with a scalpel and visualized with fluorescence microscopy. All piglets were euthanized following terminal biospies after a month had passed. All animal

experiments and care were approved by the Institutional Animal Care and Use Committee (IACUC protocol #00030454) of Children's National Medical Center and were in accordance with the "Guide for Care and Use of Laboratory Animals" published by the National Institutes of Health (National Institutes of Health publication 85-23, revised 1996).

2.2 Results

2.2.1 Scanning Electron Microscopy/Energy Dispersive X-ray Spectroscopy

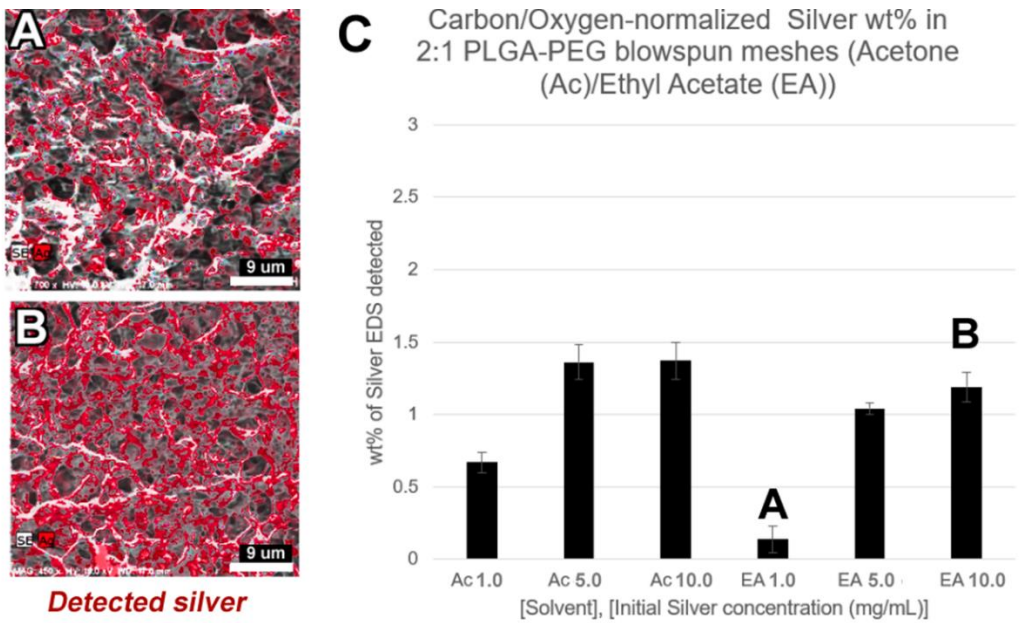

Fig 2.1: (A) Visualized SEM-EDS reading of ETAC 1mg/mL $AgNO_3$ PLGA-PEG and (B) ETAC 10mg/mL $AgNO_3$ where yellow dots indicate detection of silver. (C) Quantization of silver detected across 0-9.9 mg/mL $AgNO_3$ in either Acetone-based (Ac) or Ethyl Acetate-based (EA) blowspinning solvents. Data is normalized against zero-silver control readings.

Fig 2.1 demonstrates the difference in silver atom detection between ethyl acetate (1mg/mL silver nitrate) PLGA-PEG (Fig 2.1A) and ethyl acetate (10mg/mL

silver nitrate) PLGA-PEG (Fig 2.1B) solutions through SEM-EDS. As demonstrated in Fig 2.1C, all samples demonstrated a concentration-dependent detection of silver: Ac(1mg/mL Ag) 0.67 (±0.24) wt%, Ac(5mg/mL Ag) 1.36(±0.25) wt%, Ac(10mg/mL) 1.37(±0.18) wt%, EA(1mg/mL Ag) 0.14(±0.21) wt%, EA(5mg/mL Ag) 1.04(±0.10) wt%, EA(10mg/mL) 1.19(±0.46). Subtracting the negative control as background noise, the true silver wt% range obtained from these samples is approximately 0.18-1.37wt%.

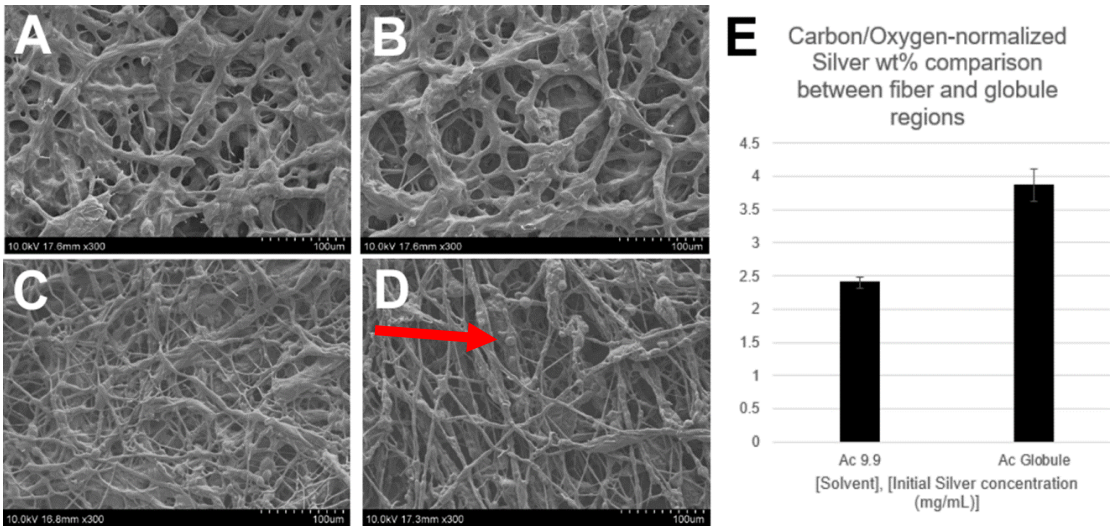

Fig 2.2.1: SEM images of nanofiber mats that were blowspun in an acetone-based solution containing (A) 0mg/mL, (B) 1mg/mL, (C) 5mg/mL, (D) 10mg/mL $AgNO_3$. (E) SEM-EDS quantification of the amount of silver detected in the globules (Ac Globule) compared to anywhere else on the nanofibers from a Ac10mg/mL $AgNO_3$ PLGA-PEG blowspinning solution.

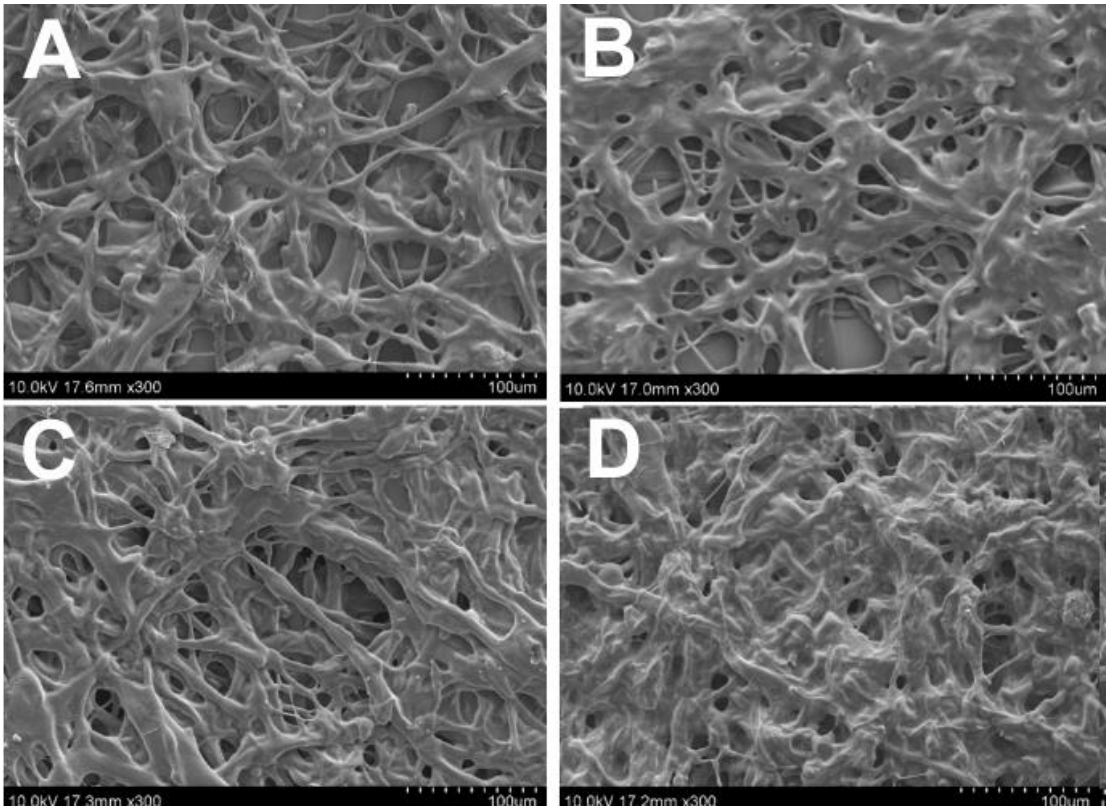

Fig2.2.2 SEM images of nanofiber mats that were blowspun in an Ethyl Acetate-based solution containing (A) 0mg/mL, (B) 1mg/mL, (C) 5mg/mL, (D) 10mg/mL $AgNO_3$.

From a morphological perspective, the 0mg/mL silver nitrate samples for both ethyl acetate and acetone resemble each other in apparent size and arrangement, though as silver wt% increases, it appears that acetone-based samples become more fibrous and begin to present globule-like structures (Fig 2.2.1) and ethyl acetate samples become more web-like and disordered (Fig 2.2.2). This could indicate differences in mechanical properties (esp. Young's modulus) or silver release rate, which were investigated (2.2.2 & 2.2.4). Carbon/oxygen-normalized silver wt% detection by SEM-EDS elicited a signal of 3.88(±0.48) wt% in the globular regions of the nanofiber mats and 2.40(±0.18) wt% elsewhere.

2.2.2 Accumulation/Release Rate of Silver

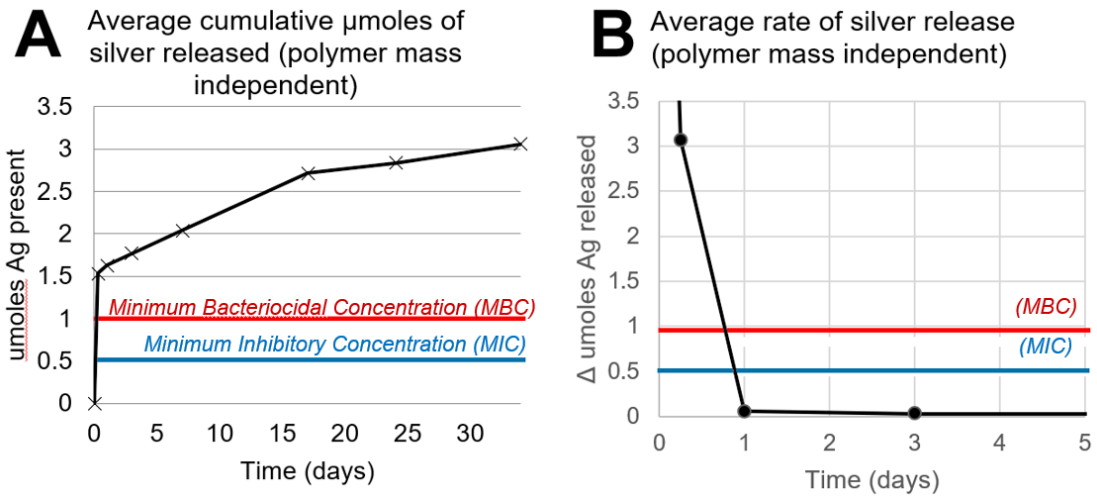

Fig 2.3: The graphical representation of (A) the *Release Rate* model of silver release and (B) the *Accumulation* model of silver release. The *Release Rate* model is the derivative of the accumulated silver in the *Accumulation* model. Each point is a Mohr titration that occurred at the x-axial time point where the y-axial amount of silver was detected in umol. The lower horizontal bar represents the silver Minimum Inhibitory Concentration (MIC) approximation and the upper horizontal bar represents the silver Minimum Bacteriocidal Concentration (MBC) approximation.

Fig. 2.3 demonstrates a preliminary study involving both *Accumulation* and *Release Rate* models discussed in methods (2.1.3) and shows a burst-like release in which half of the total released silver within the first 24 hours, followed by a slow release of the second half over the span of a month. It appears that in the *Accumulation* model Ac (10mg/mL Ag) PLGA-PEG releases a total of 3ug in 30 days, which is roughly 5x more silver than is necessary overtime (MBC~=1ug, MIC~=.5ug), and that in the *Release Rate* model, the silver release rate spends almost no time in the effective range between MIC and MBC.

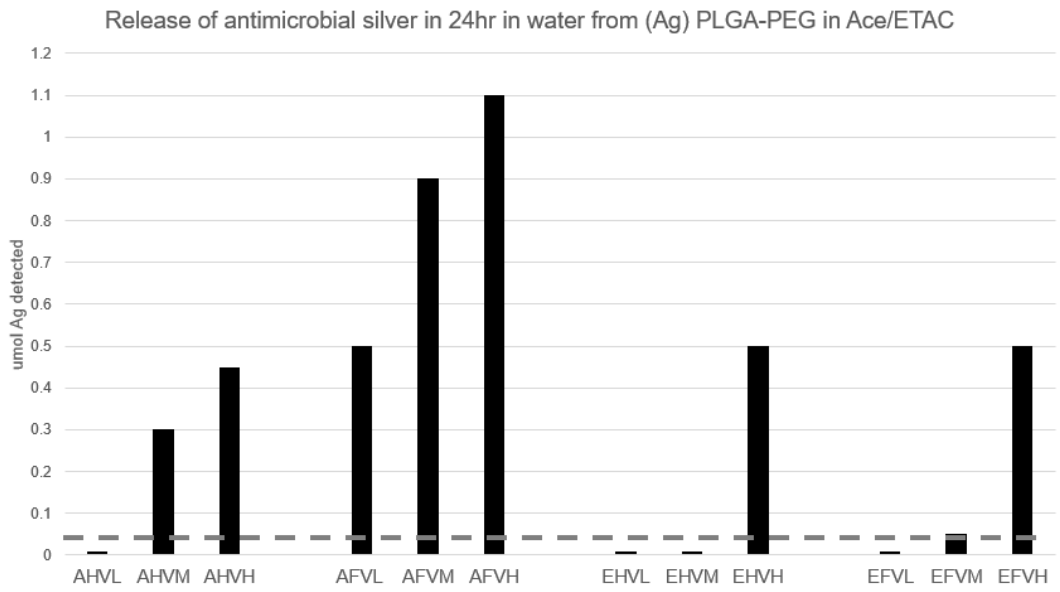

Fig 2.4: The graphical representation of the silver release array. Sample type (A = Acetone, E = Ethyl Acetate, FV = 1mL blowspinning volume, HV = 0.5mL blowspinning volume, L = 1mg/mL silver nitrate, M = 5 mg/mL silver nitrate, H = 10mg/mL silver nitrate). All measurements were made at the 24 hour timepoint. AHVL, EHVL, EHVM, EHVH, and EFVL were too dilute to detect with this titration. The horizontal bar represents the MBC approximation.

In the parameter permutation array (Fig 2.4), in which blowspinning volume, solvent identity, and silver concentration were varied for silver release optimization purposes, it appeared that the sample possesses a release profile closest to this approximated MBC (0.05umol) was EFVM (ethyl acetate, full volume, medium silver (5mg/mL)). Ethyl Acetate become the target solvent, and a new concentration range of 0.5mg/mL-5mL was selected considering the inefficient amount of silver released by EFVH. Additionally, all meshes involved in Figs. 2.3-2.4 had fully eroded within 4 weeks.

2.2.3 Differential Scanning Calorimetry

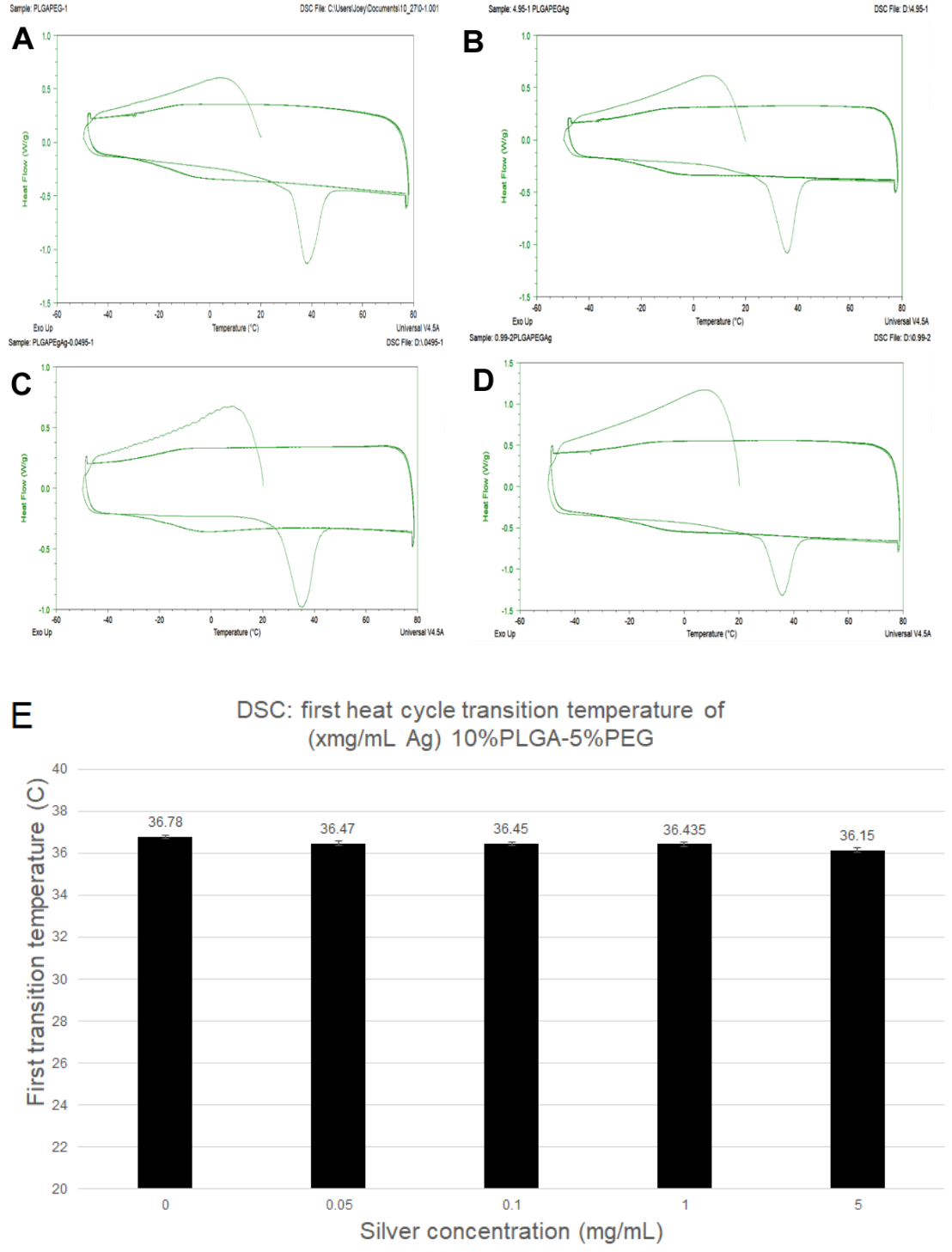

Fig 2.5: Differential Scanning Calorimetry (DSC) readings performed on ETAC (Ag) PLGA-PEG samples containing (A) 1mg/mL, (B) 5mg/mL, or (C) 10mg/mL $AgNO_3$. Heating ramp cycles performed at 20C/min. (E) Compiled melting points calculated from peak maxima computations at various $AgNO_3$ concentrations

Differential Scanning Calorimetry (DSC) revealed that following the first heating ramp cycle, all silver-containing nanofiber mats possessed a melting transition near 30-35C, comparable to nanofiber mats lacking silver (Fig 2.5). Additionally, the second heating cycle lacked a melting transition entirely, indicating that the crystalline nanofiber structure had not been restored by cooling to -40C. These findings are supported by previous *in vitro* release rate studies (2.2.2) where the nanofiber mats were observed transitioning to clear at 37°C, and also supported by subsequent *in vivo* porcine wound healing studies where the nanofiber mats transitioned within minutes of deposition (2.2.7).

2.2.4 Dynamic Mechanical Analysis

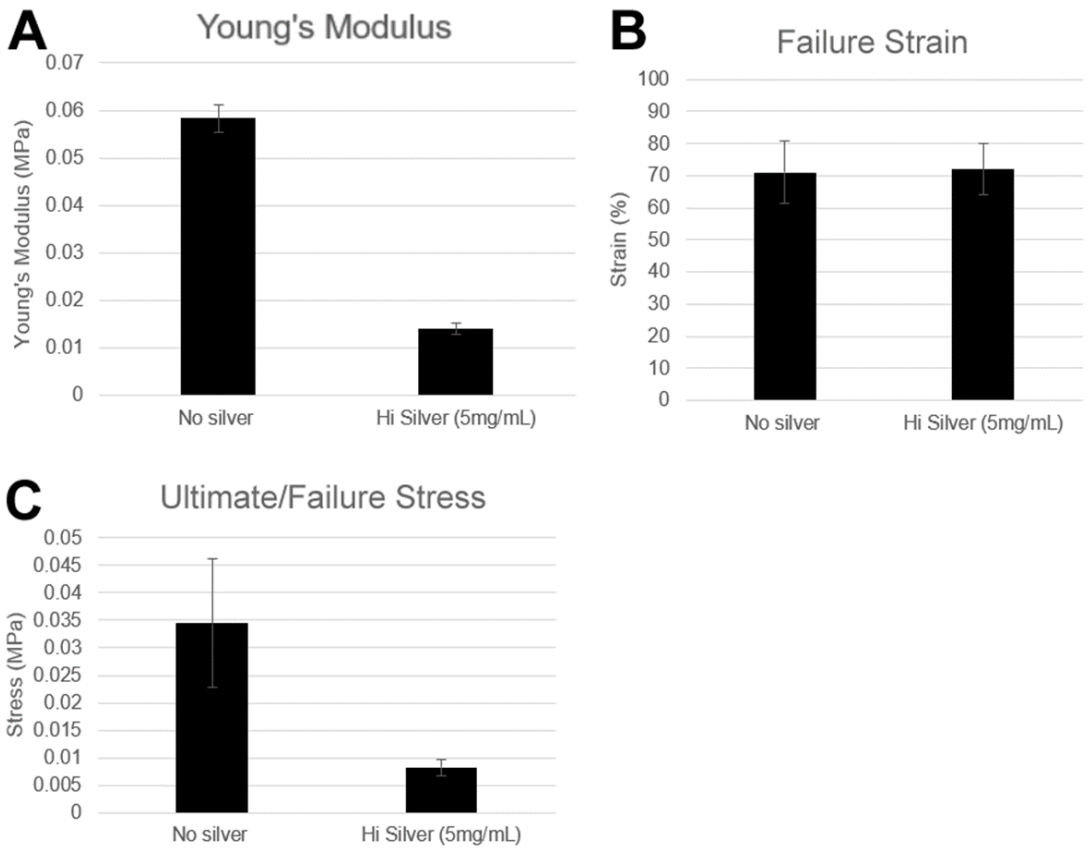

Fig 2.6: Dynamic Mechanical Analysis (DMA) performed on ETAC PLGA-PEG and ETAC 5mg/mL (Ag) PLGA-PEG. Failure recorded upon tensile failure (tearing) of nanofiber sample. Young's modulus collected at 0-5% strain.

Measurements of Young's modulus, ultimate failure stress, and failure strain via Dynamic Mechanical Analysis (DMA) indicate that the inclusion of high concentrations of silver (deemed as high concentration because it contains the amount of silver close to the upper limit of the clinically relevant range) significantly compromises Young's modulus of the nanofiber mat by about 5-fold: ETAC PLGA-PEG: 0.058(±0.006)MPa, ETAC (4.95mg/mL Ag) PLGA-PEG 0.014(±0.002)MPa (Fig 2.6). More specifically, Young's modulus is reduced by lowering the amount of stress required for the nanofiber mat to reach failure strain; compare ETAC PLGA-PEG: 0.034(±0.023)MPa and ETAC (4.95mg/mL Ag) PLGA-PEG: 0.008(±0.003)MPa. Failure strain was not significantly affected, ETAC PLGA-PEG: 71.04(±19.65)% and ETAC (4.95mg/mL Ag) PLGA-PEG: 72.07(±15.63)%.

2.2.5 Kirby-Bauer Disc Diffusion for Antimicrobial Activity

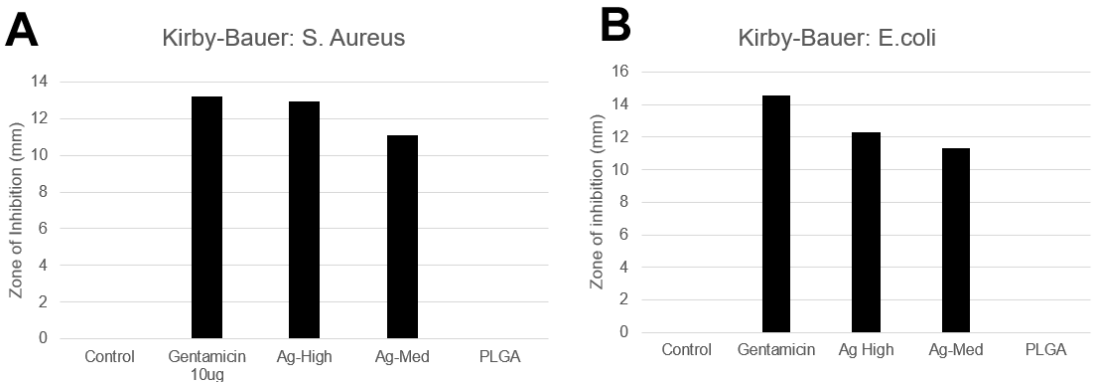

Fig 2.7: Kirby-Bauer disc diffusion Zone of Inhibition (ZOI) measurements for Gram-negative (*E. coli*) (B) and Gram-positive (*S. aureus*) strains (A). 'Control' samples were untreated gauze discs, 'PLGA' samples were discs blowspun with only PLGA-PEG. Ag-High and Ag-Med blowspinning solutions contained 1mg/mL and 5mg/mL silver nitrate respectively. No bar indicates 0mm ZOI and therefore no antimicrobial activity was detected.

Preliminary Kirby-Bauer disc diffusion antimicrobial activity studies (Fig 2.7) indicate that ETAC PLGA-PEG elicits no antimicrobial activity alone, as indicated by a Zone of Inhibition (ZOI) of 0mm. Moreover, both Ag-High and Ag-Med discs created a ZOI comparable to the ZOI of Gentamicin in both Gram-positive and Gram-negative tests. Additional tests were performed to validate our findings, but the vast majority of the silver meshes did not inhibit microbial growth in the replicate tests, as indicated by the instances of 0mm ZOI for all samples of Ag-Med and Ag-Low, and an outlier instance of 0mm ZOI in Ag-High [Disc 4 S. Aureus] (Fig 2.8.1 A). A replicate test (Fig 2.8.2) was performed using only Ag-Med, which previously demonstrated that 8 separate samples from two separate blowspinning solution batches yielded no ZOI, in which a small volume of sterile water (10uL-40uL) was transferred to the surface of the nanofiber mat discs before their placement onto the microbe-containing agar. Results demonstrate an interesting "All or Nothing" effect: all samples that received at least 30uL water yielded an antimicrobial ZOI comparable to Gentamicin. Qualitatively, there is a positive correlation between volume of water administered to the silver nanofiber mat and the likelihood that silver will be released.

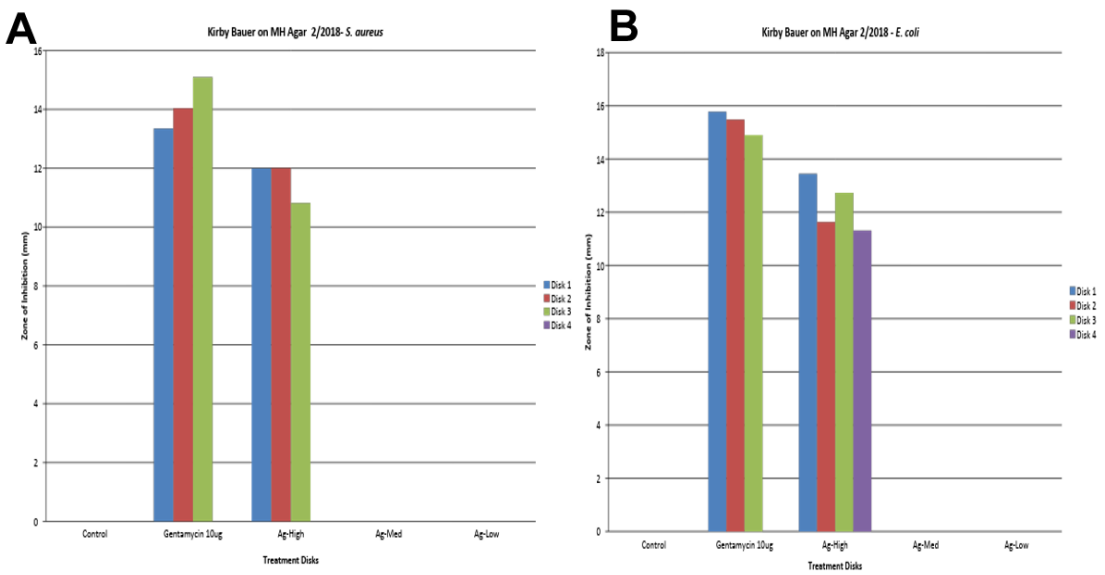

Fig 2.8.1: Kirby-Bauer disc diffusion Zone of Inhibition (ZOI) measurements performed in quadruplicate for (A) *E. coli* and (B) *S. aureus*. Ag-High: 5mg/mL, Ag-Med: 1mg/mL, Ag-Low: 0.5mg/mL silver nitrate in blowspining ETAC PLGA-PEG solution.

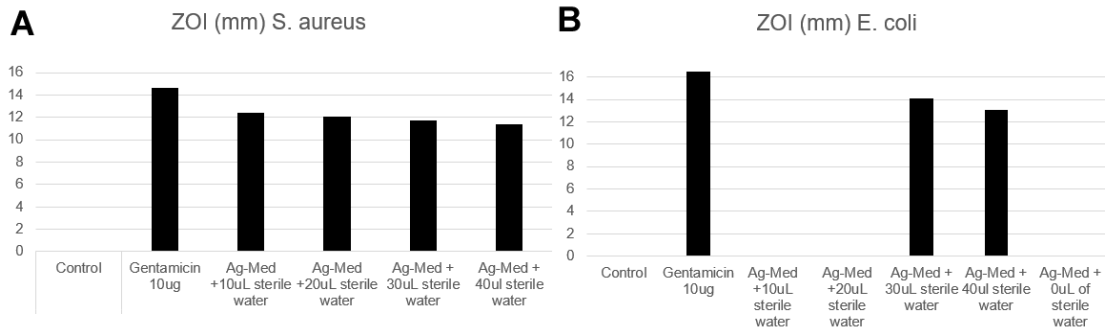

Fig 2.8.2: Kirby-Bauer disc diffusion ZOI measurements for only ETAC (Ag-Med) PLGA-PEG that were surface moistened via pipette with x-axial amount of sterile water. Measured against for (A) *E. coli* and (B) *S. aureus*.

2.2.6 MTT Cytotoxicity Assay

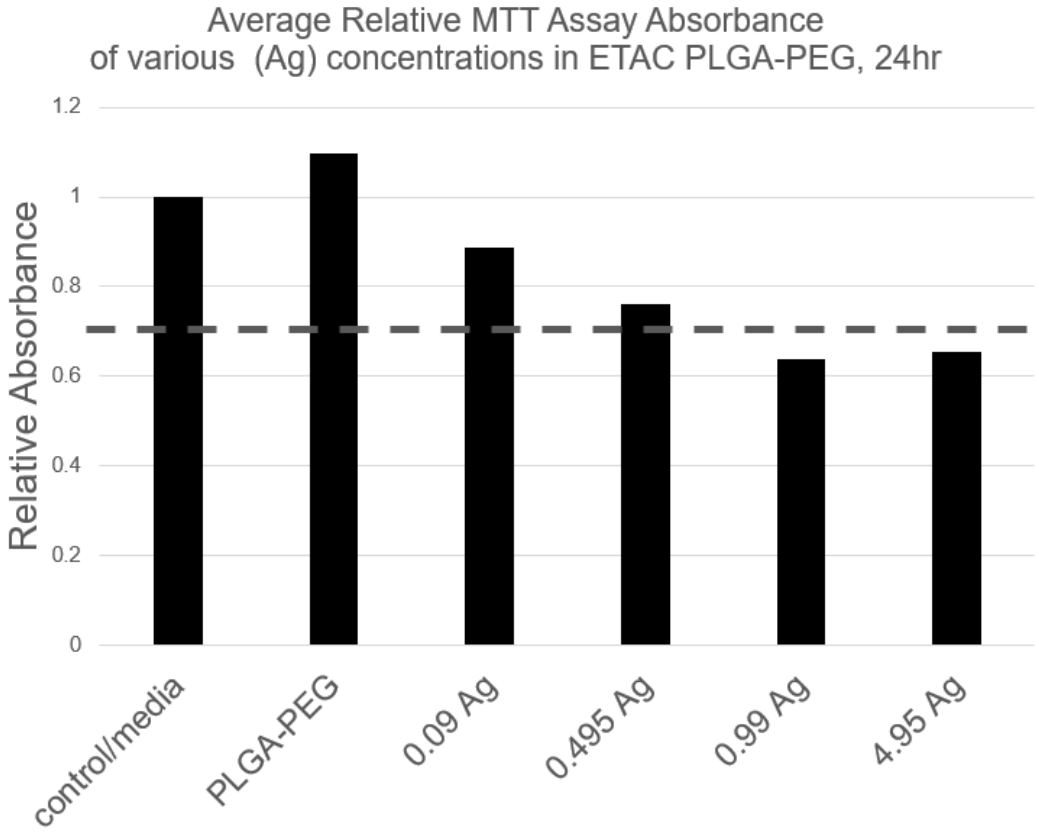

Fig 2.9: MTT assay performed on ETAC (Ag) PLGA-PEG samples blowspun onto glass slides. All fluorescence readings are normalized against control/media sample which contained only cells and media. Horizontal bar indicates target acceptable cytotoxicity.

The results were generally as expected: increasing silver concentration reduces cell survivability, and all samples were above or near the acceptable cell survivability threshold as indicated as between "mild (<50% reduced viability)" and "slight (little observable reduction in viability)" in an elution cytotoxicity assay by International Standard[30]. The PLGA-PEG sample yielding a survivability above 100% raised concern, so subsequent tests were performed to increase statistical power of the data and to possibly reveal an experimental error.

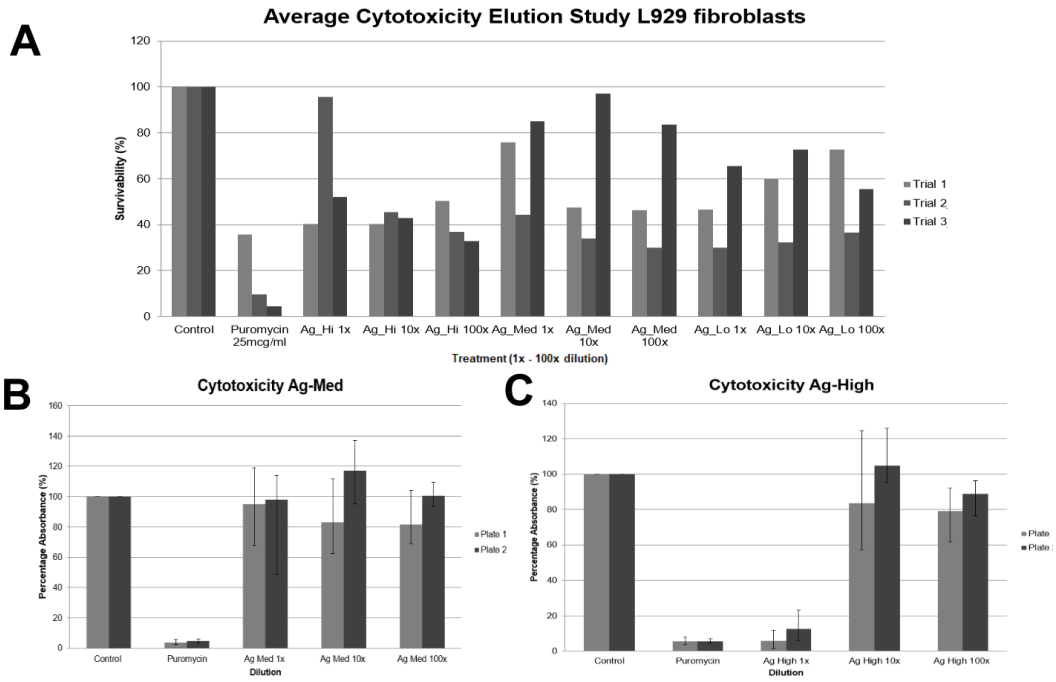

Fig 2.10: MTT assay performed on elutions of ETAC (Ag) PLGA-PEG samples blowspun onto glass slides. All fluorescence readings are normalized against control/media sample which contained only cells and media. (A) Compilation of 3 trials of ETAC (Ag) PLGA-PEG elution dilutions (1x-100x) for Ag Hi (5mg/mL $AgNO_3$), Ag Med (1mg/mL $AgNO_3$), and Ag Lo (0.5mg/mL $AgNO_3$). (B-C) Individual replicate studies for the titular sample

Replicate studies done in triplicate revealed similar data, but once again our PLGA-PEG samples presented problematic data: each PLGA-PEG batch had a sample that yielded over 100% survivability and a sample that had a significantly compromised cell survivability (<60%). Suspecting an interference in the absorbance assay by the sample itself (See more in 2.3.5), a modified MTT assay that utilizes the extracted elutions of the samples instead of the samples themselves was implemented (Fig 2.10). Dilutions of this elutant were performed over the range of 1x-100x. Again, we saw instances of PLGA-PEG demonstrating unexpected toxic behavior, and the remaining data for the silver samples is difficult to interpret in respect to discerning whether or not the sample yields a cell survivability above the minimum threshold. It is possible,

however, to make general, relative comparisons between the samples: there doesn't appear to be an obvious, dramatic penalty to cell survivability between the highest concentrations of silver and the lowest. Finding that the silver samples did not have an obvious toxic limit within our samples, another approach was used to further understand the effect of silver on cell survivability (and therefore, wound healing).

2.2.7 Porcine *in vivo* Wound Healing

As mentioned previously in the mechanical analysis of the silver dressings, the mechanical properties, especially the Young's modulus, are affected by the presence of silver. However, even as the piglet rolled about or rubbed its back against the walls of the cage, no silver dressing ever fell off, tore, or otherwise mechanically failed over the span of the month on any of the completed studies. An unexpected positive property of the nanofiber mats containing silver was that they had a 'sticky' texture, a sign that the nanofiber mats possessed stronger adhesive capabilities than standard PLGA-PEG. Additionally, the nanofiber mats were opaque while being blowspun, and transitioned to clear shortly afterwards, while adjusting to body temperature. Assessing wound area approximations, diagnostic reports on dermal biopsies, and qualitative appearance of the wounds over time, it was determined that wounds treated with silver nanofiber mats qualitatively did not appear to heal significantly slower than the wounds with any other treatments, exception to some Tegaderm samples. In some instances, silver nanofiber mats appeared to improve wound healing when compared to untreated wounds or wounds covered by PLGA-PEG (Fig 2.11). Additionally, there was no discernable

difference between wounds treated with low concentrations of silver and those treated with high concentrations (both within the clinically relevant range) (Fig 2.12).

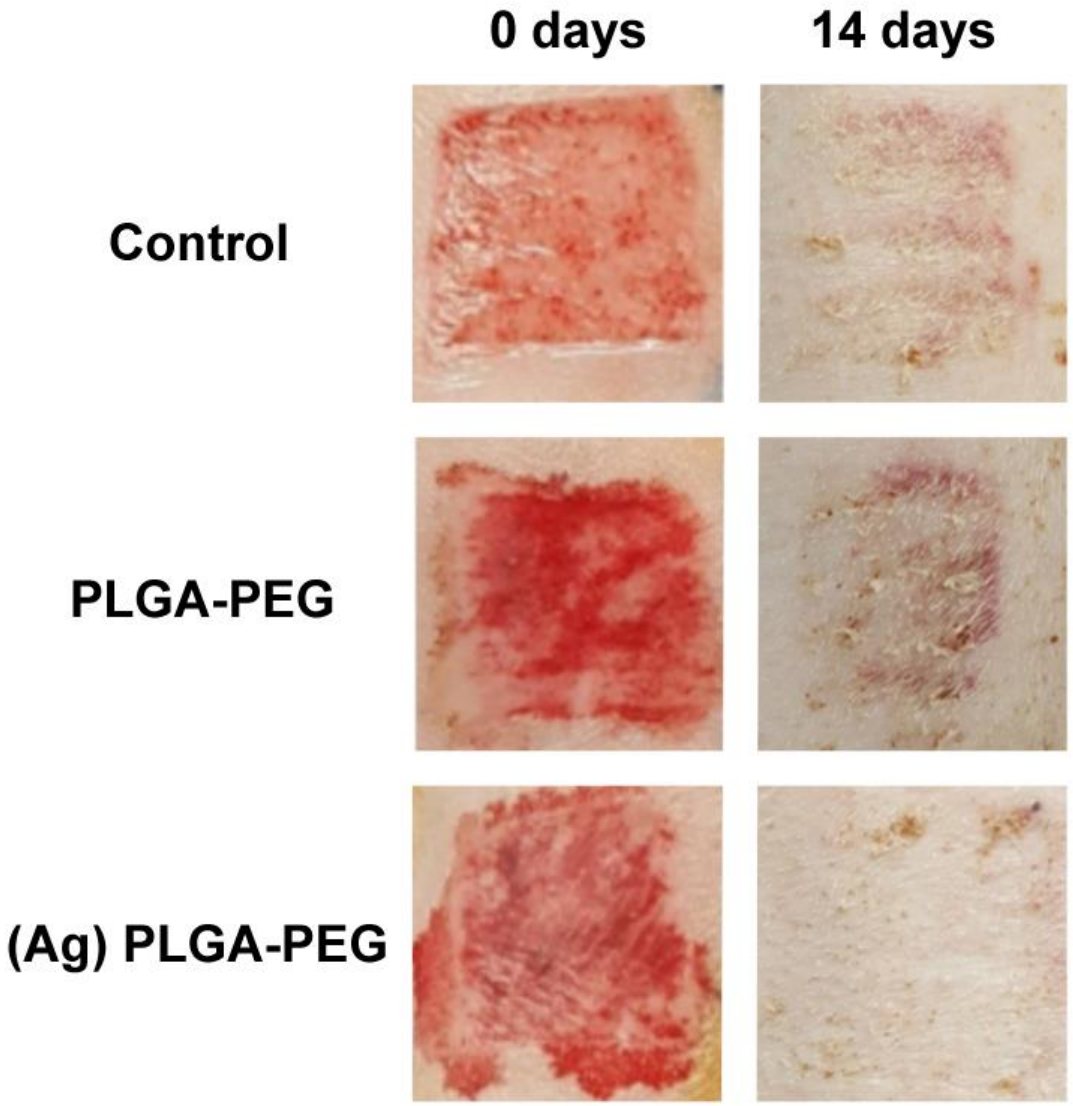

Fig 2.11: Porcine *in vivo* wound study photographs: 0-day sample images were collected immediately after wound simulation and before coverage. 14-day images collected after lightly scraping off scar tissue and debris. ((5mg/mL) Ag) PLGA-PEG appears to have the least traumatic skin surface.

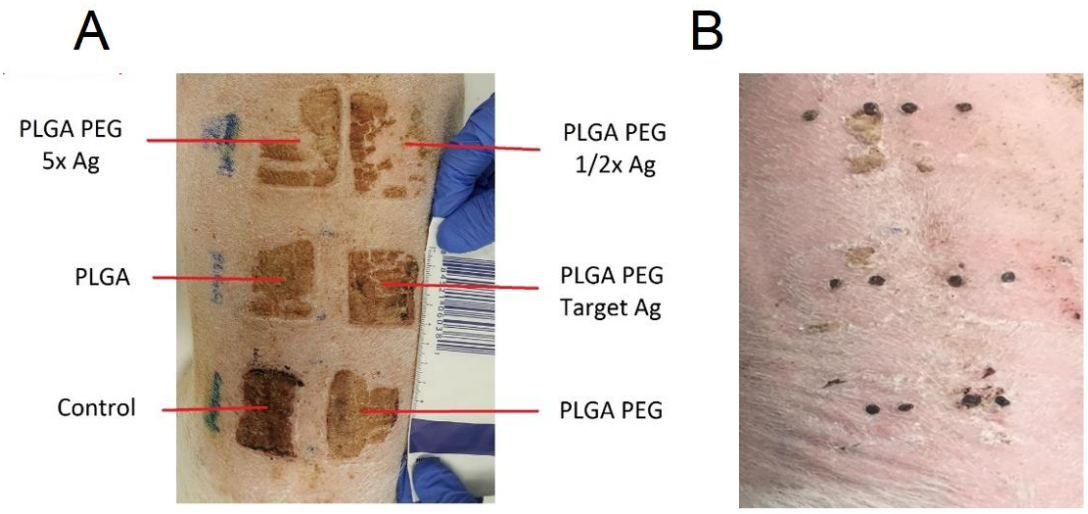

Fig 2.12: Secondary porcine *in vivo* wound study photographs taken from a different piglet: (A) Photograph of various wound treatments after 1 week of healing. PLGA-PEG 5x Ag = (5mg/mL $AgNO_3$), PLGA-PEG Target Ag = (1mg/mL $AgNO_3$), and PLGA-PEG 1/2x Ag = (0.5mg/mL $AgNO_3$). (B) Same injuries from 2.11A 3 weeks later. Black spots are previous biopsy sites.

The scab that forms from wounds covered by PLGA-PEG/(Ag) PLGA-PEG appears beige in color, compared to the dark brown hue of untreated wounds, and there is no obvious sign of polymer present in the skin beneath the scab (Fig 2.12, compare Control to any other sample). Subsequent biopsy analysis (2.1.8) reveals that this color difference is due to PLGA-PEG, which is present solely in the scab. This is indicated by the ubiquitous fluorescence of the scab tissue, and the absence of any non-background fluorescence anywhere beneath the scab-skin interface (Fig 2.13). This is made more obvious by top-down views of the scab alone, and the sub-scab dermal tissue alone. Additionally, the hypodermal region, which would be entirely inaccessible by PLGA-PEG, presents the same fluorescence intensity as the top of the

epidermal region, also implying that there is no PLGA-PEG incorporated into the skin beneath the scab.

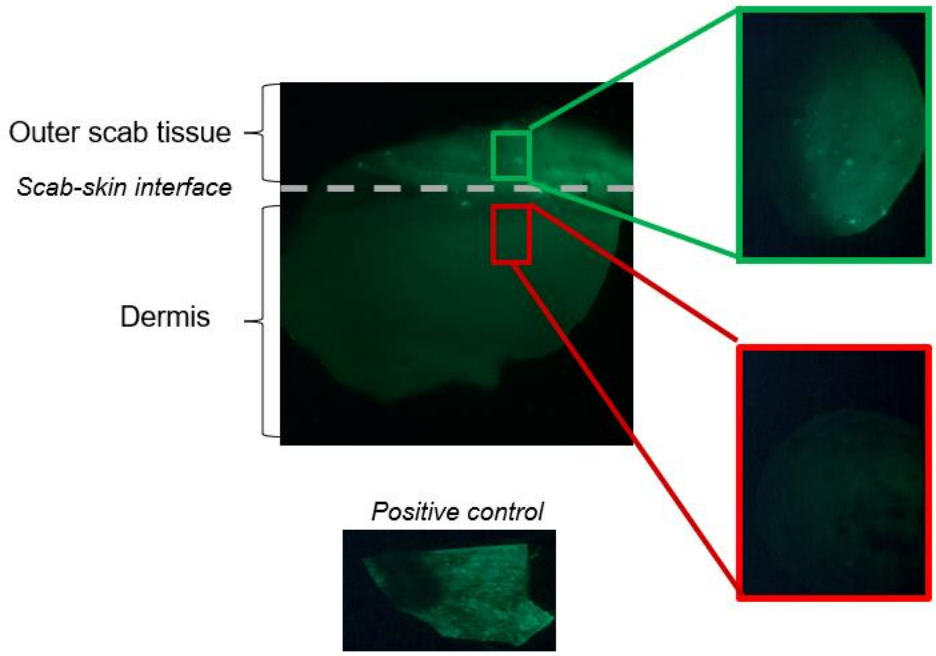

Fig. 2.13: Cross sectional fluorescence microscopy of biopsy of *f*-PLGA-PEG treated wound. Positive control is a raw fragment of PLGA-*f* imaged at the same exposure and settings. The green box is a top-down image of the scab+dermal biopsy. The red box is the top-down image of the dermal biopsy with the scab removed.

2.3 Discussion

2.3.1 Scanning Electron Microscopy/Energy Dispersive X-ray Spectroscopy

The concentration of silver incorporated into currently available silver dressings tends to be highly variable, but averages around 1% silver by weight, and generally contains more silver than would be necessary or even released[26]. The first objective therefore was to demonstrate that silver can be incorporated into the blowspinning solution and delivered in a concentration-dependent, evenly distributed manner into the resulting nanofiber mat at a concentration of approximately 1 wt% silver. Additionally, it would

be important to characterize the nature of silver deposition (coating, impregnation, spread, particulate aggregation, etc) because these factors control the rate and profile of silver release. An aqueous release study at this point would not prove effective because it is common for only a fraction of silver to be released from its dressing in aqueous conditions, and a thermal analysis would be ignorant of homology or spatial arrangement, so instead, Scanning Electron Microscopy Energy-Dispersive X-ray Spectroscopy (SEM-EDS) was utilized to understand the quantity, arrangement, and any potential localization. Estimating the target dry mass ratio of blowspinning solution to silver to be about 0.5 wt% - 1.5 wt% (i.e., counting PLGA and PEG weight, excluding dispersive acetone), 0.99mg/mL – 9.9mg/mL silver nitrate PLGA-PEG solutions were mixed and blowspun in acetone and ethyl acetate, two prospective solvents. Acetone was previously studied as a SBS solvent, but ethyl ecetate can dissolve 5-fold more silver salt, so both were evaluated at this stage. Non-EDS images were also collected through standard SEM for morphological characterization for insight into possible mechanical or structural changes—it is important that silver does not compromise the key features of blowspun PLGA-PEG (Elastic, conformal, sprays opaque but melts to clear at 31C, degradable). Preliminarily, SEM-EDS and SEM imaging demonstrates that the amount of silver that results in the nanofiber mat can be controlled by the amount of silver included in the original blowspinning solution over clinically relevant ranges, as indicated by the significantly increasing detection of silver as initial silver concentration increases (Fig. 2.1C). Across all EtAc samples, silver was homogeneously distributed across the entire surface and at each layer (ex. Fig 2.1A-B), implying silver salt had indeed been incorporated successfully into

blowspinning solution, and is deposited at a constant rate as nanofibers are blowspun. Subtracting the noise from the negative controls as a baseline, the silver wt% range demonstrated in Fig 2.1C is 0.18-1.37wt%, effectively encompassing the majority of typical silver dressing weight contents (0.1%-1.5%). Therefore, blowspun nanofiber mats can contain silver at clinically relevant concentrations. Acetone solvent samples presented silver-rich globule structures as silver concentration increased (Fig 2.2.1D), but the globules were dispersed homogenously throughout the nanofiber mat, and non-globular silver presence was also homogeneous. Interestingly, the differences between the resulting fibers tend to vary depending upon both the solvent used and the quantity of silver present. Though viscosity of the two solvents is different, the two 0mg/mL silver nitrate samples lacking any obvious differences from each other suggest that silver solubility plays a prominent role in the structure of the resulting nanofiber mat. Because silver salt is less soluble in acetone, it may be more likely to form silver-rich particulates with polymer that act as nanofiber deposition anchors, which is supported by EDS images that detected nearly twice as much silver in the fiber-attached globules than anywhere else in the mesh.

2.3.2 Accumulation/Release Rate of Silver Subsection

After demonstrating that silver is indeed present in the blowspun nanofiber mat, the release profile of silver from the mesh must be known to show that silver is not fixed to or shielded by the polymer fibers and will freely experience aqueous ionization to release silver in solution: Silver dressings are often used for even minor burns, which can be exudative for up to 72 hours[31], readily creating the aqueous environment for

dressings to donate Ag+ ions. The time-dependent Mohr titration was performed to understand the profile of silver release in a preliminary study that observes two devised models (Fig 2.3): *Accumulation* is the sum of the Ag released at each time point, which tracks the amount of silver released as it accumulates in solution. This approach appreciates lingering silver and assumes that any silver that was released at any time is still present and active within the wound bed. This is valid because topical application involves slower clearance than internal deposition, and silver has been observed to maintain potency, even after killing a microbe[32]. *Release Rate* is the derivative of this curve. After implantation, eluted silver is constantly being exchanged with the wound exudate and does not accumulate at the wound site. This model appreciates highly exudative wound beds or rapidly cleared silver. The concentration recorded for both models at each time point was then converted to a μmol measurement to be volume-independent, because wound exudate volume can be highly variable and "volume" of a wound bed can be incredibly subjective, both of which would cause a volume-dependent measurement to poorly represent the actual quantity of silver released. This volume-independent value was then compared to volume-independent approximations of MIC and MBC. Experimentally, MIC represents the bottom limit for effective silver release, because any less is ineffective at preventing a microbial colonization from worsening, and MBC represents the upper limit because once all microbes have been killed, any additional silver would cause unnecessary cytotoxicity. As mentioned in the results, both models spend very little time within this effective range: The silver *Accumulated* quickly reaches nearly two-fold more silver than is necessary to accumulate in the wound bed within 24 hours, and the silver *Release Rate* is either too

high early on or too little later, for all except for a few hours during the first day. To optimize silver release, less silver should be released in total, and the burst of silver should be less dramatic (i.e., less steep *Release Rate* and *Accumulation)* to allow for a more prolonged, controlled, effective release rate over time. Although these models use several approximations (e.g., wound bed volume, estimated MIC/MBC, amount of mesh present per wound bed area, etc), the observations that less silver needs to be released and more gradually held true. As discussed in the SEM-EDS section, ethyl acetate lacked obvious silver globule formation, most likely to silver possessing a 5-fold solubility in ethyl acetate compared to acetone. It therefore seemed likely that if silver formed fewer particles and more readily dissolved in ethyl acetate, that it would be more homogeneously distributed and trapped within the weblike nanofibers, experiencing aqueous ionization slower than surface-exposed silver-rich particulates on acetone mats, despite the silver wt% of the two solvent types being the same (Fig 2.1C). The conclusion that acetone-based blowspinning solutions generate nanofiber mats that more rapidly release silver was found to be correct: a 24-hour timepoint release study (Fig 2.4) demonstrates that although acetone and ethyl acetate samples contain the same amount of silver in the blowspinning solution, acetone-based samples will release more silver during the burst. This difference becomes more obvious at higher silver concentrations. Additionally, ethyl acetate samples did not release twice as much silver once the volume of blowspinning solution used was doubled, even though this behavior was present in acetone-based samples. This is an interesting observation, because Ethyl Acetate Full Volume High Silver (EFVH) contains twice as much silver by mass than Ethyl Acetate Half Volume High Silver (EHVH) does, even

though the wt% of silver is the same between the two. This can be possible because the same total surface area of fiber mat was exposed to the aqueous environment between each sample (because the meshes were spun onto glass slides of the same size), so the diffusion rate was the same despite there being more silver contained within the sample. The differences in silver release would then be likely to manifest later, as the total silver released of EHVH would likely be half of EFVH in the following month. This has attractive properties, because this suggests that Ethyl Acetate-based blowspinning solutions result in nanofiber mats that can throttle silver release, independent of the thickness of the resulting fiber mat. Additionally, all meshes had fully eroded within 4 weeks, suggesting aqueous degradability was not influenced with the addition of silver.

2.3.3 Mechanical/Thermal Properties

It is important to evaluate the mechanical properties of the fiber mats over the clinically-relevant silver concentration range (which was found to be roughly 0.495mg/mL-4.95mL $AgNO_3$ in the release rate studies) to ensure that silver does not dramatically hinder the properties that give blowspun PLGA-PEG advantage over current available silver dressings. The most important of which are (i) The ability of PLGA-PEG meshes to experience a melting transition at 31C (ii) The ability to appear opaque while being blowspun and transparent after melting (iii) The ability to be wound-adhering and elastic. Regarding the melting transition— 31C is a very practical temperature for the PLGA-PEG to transition: it is considerably higher than room temperature and slightly lower than typical body temperature. Unacceptable

interference by silver would involve the melting temperature climbing above 37°C, falling below 23°C, or disappearing entirely. Neither instance of unacceptable interference was observed, and all samples stayed within the approximate 30-35C range (Fig 2.5). This suggests that there is no dependency of the melting transition on silver presence or concentration, and as confirmed qualitatively during *in vivo* porcine studies (2.2.7), silver meshes are blowspun opaque and transition to clear. Regarding the elastic ability of the wound dressing, it was likely considering the obvious conformational differences between silver-containing and non-silver-containing nanofiber mats that silver could have significant effects on mechanical properties of the resulting mats. This was found to be generally true, as meshes containing high (clinically-relevant) concentrations of silver have 5-fold compromised Young's Moduli and failure stresses (Fig 2.6). This meant that compromised elasticity was another penalty to consider while selecting the ideal silver concentration, in addition to cytotoxicity. The compromised properties ultimately were not dramatic enough to cause any mechanical failure of nanofiber mats containing high concentrations of silver in the subsequent *in vivo* porcine wound healing study, as discussed in section 2.2.7. The difference in rigorousness between a sedentary, cooperating human patient and an uncooperating piglet allowed to rub and scratch its back is also relevant in this case.

2.3.4 Antimicrobial Activity

Once it was asserted that clinically relevant concentrations of silver would not significantly interfere with the desirable properties of PLGA-PEG nanofiber mats, such as melting to clear at ~37°C and degrading in approximately 4 weeks, the next

step was to evaluate the antimicrobial and cytotoxic properties of the nanofiber meshes containing silver. A typical broth microdilution assay would not be an accurate model, as the silver dressings typically will not be fully submerged, and only one side of the silver dressing will be directly in contact with the wound bed. Instead, a Kirby-Bauer disc diffusion test was determined to be the most effective model available, most practically replicating an interfacial deposition of silver between two moist (but not submerged) surfaces to measure antimicrobial efficacy. Silver has been found to possess broad spectrum antimicrobial activity, so both treatments were tested against Gram positive (*S. aureus*) and Gram negative (*E. coli*) strains to demonstrate this range. It is worth mentioning that, as previously discussed (See: Background), silver is also effective against fungal and drug resistant infections. This includes MRSA and other heavily antibiotic resistant nosocomial infection-inducing microbes, which are incredibly relevant to the current antibiotic-resistant infection crisis[9,16]. The antimicrobial effectiveness of silver against these strains has already been well described[17], so in this test we simply demonstrated that the two most relevant and differing subsets of microbes (Gram-positive and Gram-negative) are susceptible to released silver. Both Ag-High and Ag-Med discs created a ZOI comparable to the ZOI of Gentamicin, indicating comparable antimicrobial activity against both Gram-positive and Gram-negative microbes (Fig 2.7). Additional tests were performed to increase the statistical power of these findings, but the vast majority of the silver meshes did not inhibit microbial growth in the replicate tests, as indicated by the instances of 0mm ZOI for all samples of Ag-Med and Ag-Low, and an outlier instance of 0mm ZOI in Ag-High [Disc 4 S. Aureus] (2.8.1). This is

especially interesting, because a parallel cytotoxicity test was run (2.2.6) in which all silver samples from the same batch possessed silver toxicity. At this stage it was already confirmed that silver is indeed present in all discs (2.2.1-2.2.2), that the silver is released at antimicrobial concentrations in aqueous solutions (2.2.2), and that the silver that is released is active (2.2.5). The only room for doubt was in whether the silver was released from the discs. The most likely cause for the 0mm ZOI was that the agar-disc interface was not moist enough for ionize silver and release it from the nanofiber mat. To test this hypothesis, a replicate test was performed using only Ag-Med, which previously demonstrated that 8 separate samples from two separate blowspinning solution batches yielded no ZOI, in which a small volume of sterile water (10uL-40uL) was transferred to the surface of the nanofiber mat discs before their placement onto the microbe-containing agar. Qualitatively, there appears to be a positive correlation between volume of water experienced by the silver nanofiber mat and the likelihood that silver will be released, confirming the finding that silver meshes tend to be more successful in moist wound beds or highly exudative interfaces[26]. Silver dressings are already well known to be more effective in moist wound beds, such as exudative wounds caused by even superficial burns, so it is likely that our original agar model was not true to a real burn wound by lacking moisture. In the event of a dry wound in need of silver dressings, it may be possible to administer sterile water to the would before or after coverage with ETAC (Ag) PLGA-PEG.

2.3.5 Cytotoxicity

Silver has known cytotoxic activity as a result of its broad spectrum antibiotic activity, and although silver is significantly more toxic to microbes than to mammalian cells, it is critical that the optimal balance is found between antimicrobial activity and toxicity-induced cell death: Because these silver nanofiber mats ultimately will serve to expedite burn wound treatment, it is important that re-epithelialization and wound clearance are not hampered by cytotoxicity. Approaching the test, a relative absorbance of MTT solution (and thereby, cell survivability) of approximately 65%-70% is the acceptable minimum to be comparable to cell survivabilities of clinically approved silver dressings. This metric ultimately was not usable because of the unusual standardization of the test and the data produced by it: PLGA-PEG has been found previously to be nontoxic to cells[23] and is widely used as a biocompatible polymer, but there are several instances within our data (2.2.6) that indicate otherwise. So it is unlikely that the data presented by these samples is accurate in any non-relative basis: it most likely overestimates the toxicity of the silver dressings as it does PLGA-PEG potentially due to some physical cytotoxicity caused by mats putting pressure on cells or inhibiting O2 exchange across the sample slides, or because PEG contained within the samples is enough to be toxic when fully submerged in small volumes (though this would not happen *in vivo*). Comparing detected cytotoxities on a relative basis, there does not appear to be any meaningful difference in cell viability between samples with high concentrations of silver, samples with low concentrations of silver, and samples that contain only PLGA-PEG (Fig 2.10). The only exception to this is Ag-Hi 1x dilution, which is most likely an overestimate of toxicity: cytotoxity tests were

performed under fully submerged conditions, which were found to dramatically expedite the release of silver (2.2.5). Ultimately, the ideal silver concentration would have the highest antimicrobial activity with the lowest possible cell viability detriment, so finding that the clinically relevant range of silver concentration has comparable cell survivabilities would allow for higher concentrations of silver to be used. This is already reflected in currently available silver dressings that flood the wound with more silver than is necessary with little detriment[26]. Future methods involving interfacial contact between the nanofiber mat and a confluent layer of fibroblasts (e.g. some air-media cytotoxicity assay) would most likely generate a more realistic profile of expected cytotoxicity.

2.3.6 Wound Healing and Fate Tracking

On the basis of visible skin trauma, scarring, redness, and wound size over time, there was no discernable difference between wounds treated with lower concentrations of silver and those treated with higher concentrations (both within the clinically relevant range), supporting our previous finding that there does not appear to be a significant toxic penalty to using nanofiber mats that contain high concentrations of silver and are therefore more effective as antimicrobial agents. This is promising evidence, because this test was performed in the absence of intentional microbial bioburden: there were no signs of any wound, including the uncovered wounds, becoming infected, and therefore the wound healing process was only measurement of healing promotion/toxicity, not antimicrobial activity. Silver dressings are known to be cytotoxic and are currently only used in the presence or suspicion of infection and

have been claimed to slow healing otherwise[26], but here it is demonstrated that blowspun (Ag) PLGA-PEG may even outpace untreated wounds in terms of rate of wound healing, which may open opportunities to utilize (Ag) PLGA-PEG in situations with low/no risk of infection: If there is little penalty to using (Ag) PLGA-PEG silver dressings when there is no infection, it begs the question of why a silver nanofiber mat should ever not be used to prevent potential subsequent or nosocomial infection, especially in light of the fact that the vast majority of burn-related deaths are due to infection (1.1). If this test was performed in the presence of bioburden, as demonstrated by the previous Kirby-Bauer disc diffusion test, (Ag) PLGA-PEG would be expected to elicit antimicrobial activity in the area underneath and near the dressing, and the advantage to using silver in these nanofiber mats would be much more obvious—any non-antibiotic treatments would likely result in infection-induced wound trauma that dramatically slows the healing process more severely than the presence of silver would. As such, it would be a promising future study to investigate a wound healing model that appreciates bioburden, and if possible, uses MRSA or other modern and relevant microbes as the model infectious agent. The immediately next step in this experiment, however, was to determine the fate of the blowspun nanofiber mat to confirm suspicion that it degrades/exits the wound bed through scab tissue. The scab that forms from wounds covered by PLGA-PEG/(Ag) PLGA-PEG appears beige in color, compared to the dark brown hue of untreated wounds (Fig 2.12A), and there is no obvious sign of polymer present in the skin beneath the scab, so it was likely that PLGA-PEG becomes incorporated into the scab and eventually falls off. To verify this suspicion, the fluorescence fate study was performed, in

which it was determined that there is no dermal deposition of polymer, and all PLGA-PEG instead is incorporated into scab tissue that falls off of its own accord (2.2.7). Therefore, it is very likely that once all scab tissue is removed or falls off, there will be little to no (Ag) PLGA-PEG remaining at the wound bed. This is another unexpected positive trait: scab formation is indicative of wound healing and is evidence that the wound bed is becoming less immune-compromised as the body naturally repairs itself, so at this point, silver and PLGA-PEG would both be unnecessary at the wound bed, and should be either degraded or removed; ideally, the (Ag) PLGA-PEG would be incorporated into the scab tissue, which falls off readily with time.

Additional: Chapter 3: Brillouin Microscopy as a non-contact method of insight into mechanical properties of materials

3.1 Introduction

3.1.1 Brillouin Imaging

Brillouin imaging is a label-free, confocal-compatible, non-contact technique of 2D/3D mechanical imaging with subcellular resolution[33]. The Brillouin light-scattering interaction with sample material produces a measurable spectral frequency shift, which can be correlated to the longitudinal modulus of the material[34]. This modulus may or may not be directly linked to known mechanical properties (Young's modulus, tensile modulus, etc.), though it has demonstrated sensitivity to biomechanical changes in

living systems[34]. Brillouin imaging has great potential in biomechanical analysis of living tissue where contact-based measurements are discouraged, such as corneal diagnostic monitoring[35]. To achieve this potential, an important step would be to correlate longitudinal modulus determined from Brillouin imaging to a more tangible, further-understood and investigated mechanical measurement, such as Young's modulus. Some correlations have been made previously, though with error bars that encompass orders of magnitude[36]. Attempts to further understand what exactly influences Brillouin light scattering, such as the states of present water (3.1.2), may provide insight into translating longitudinal modulus into other measurement methods.

3.1.2 States of water in hydrogels

Hydrogels are networks of hydrophilic polymer chains that contain a high percentage of water by vol.%, though not all of this water exists in the same "state" within the hydrogel. There are several different ways of classifying these states, a common method of which being: determining the free/bound and freezing/nonfreezing states of water on a composition basis. This results in three primary categories of water in a hydrogel: (i) free and freezing(FF), (ii) bound and freezing(BF), and (iii) bound and nonfreezing(BnF)[37]. On a physical basis, these groups can be distinguished from each other based on their individual phase transition behavior, particularly their freezing behaviors. FF water will form stable, typical hexagonal crystalline ice structures, while BF water will form metastable or amorphous ice as a result of water-polymer interaction. BnF water will not form ice, due to physical separation or interaction-disruption of neighboring water molecules by hydrophilic polymer[37]. To experimentally distinguish between these classes of water, Differential Scanning

Calorimetry (DSC) can detect the melting/freezing transitions of FF water at 0C and a shifted transition of BF water. In case of peak overlap, deconvolution algorithms may be used to separate the two peaks. To quantify BnF water, the freezing water content can be subtracted from total water content (determined by drying the gels into a water-devoid state and measuring the change in mass), resulting in the percentage of water present within the gel that did not participate in melting/freezing transitions.

3.1.3 Experimental Design

In the interest of generating preliminary data to attempt to gain insight into what parameters Brillouin imaging considers when producing a longitudinal modulus measurement, polyacrylamide gels are attractive test samples due to their simple and rapid manufacturing protocols, broad range for possible stiffnesses, demonstrated and understood FF + BF + BnF water states, and their transparent nature (Brillouin imaging works best on clear samples). Because it is possible that Brillouin light scattering could be influenced by phonic feedback of polymer density, water states, or degree of crosslinking, all three properties were varied in a permutation array of samples. A comparative study was devised in which the mechanical properties of hydrogels with varying composition parameters are interpreted by Brillouin imaging and Dynamic Mechanical Analysis (DMA), and the readings between each test would be fit together to attempt to correlate longitudinal modulus to Young's modulus. Hydrogel samples would also be measured for their water content through DSC and desiccation. Hydrogels would be analyzed in order from least destructive to most destructive

techniques, being: (1) Brillouin imaging, (2) DMA, (3) DSC, to assure that each analysis method is effectively measuring the same properties.

3.2 Methods

3.2.1 Hydrogel manufacturing

60% PBS-based polyacrylamide solutions (40% Acrylamide and 2% bisacrylamide solution mixed in 2:1) are initiated with ammonium persulfate and TEMED. For permutation arrays, polyacrylamide solutions are selected from the below table, and/or bisacrylamide is concentrated up to 4-fold (2-8% in original acylamide/bisacrylamide solution).

~Final Acryl Conc.	5%	6%	8%	10%	12%	14%	15%	16%	20%	25%
Acryl/Bis	187.5	225	300	375	450	525	562.5	600	750	937.5
60%PBS	812.5	775	700	625	550	475	437.5	400	250	62.5

All values in uL

After gelation initiation with TEMED, 50-100uL of polyacrylamide solution is loaded by pipette into needleless syringes (BD 1mL Tuberculin Slip Tip) stored upright with the top bottleneck removed by razorblade. After gelation has completed, the gels are ejected by depressing the syringe plungers.

3.2.2 Dynamic Mechanical Analysis

The entire gels (~3mm thick x 5mm diameter) are loaded for compression Dynamic Mechanical Analysis (DMA) analysis: Strain sweep methods were used to obtain the Young's Modulus of all gel samples after Brillouin imaging and before DSC. 5%-10% strain was used as the linear region from which Young's modulus was obtained.

3.2.3 Differential Scanning Calorimetry

A piece of each hydrogel (7-13mg in weight) was removed by razorblade and sealed in an aluminum hermetic pan. Differential Scanning Calorimetry (DSC) was performed in a 4-cycle heating ramp (to ensure accuracy of findings) at 5C/min from -65C to 60C. Free water should have a peak near 0C, bound water the other, nonzero peak. Nonfreezing water will not be visible in DSC. Integration of these peaks and multiplying by grams of sample, then dividing by 333 J/g of water will result in the grams of water detected at that peak. Deconvolution may be necessary in case of peak overlap.

3.3 Discussion of prospective data

3.3.1 Mechanical correlations to Brillouin Modulus

Early impressions of the data indicate a conserved positive relationship between Young's modulus and Brillouin shift/longitudinal modulus. In Fig 3.1A, increasing polyacrylamide concentration (and thereby, the Young's modulus) results in a strong linear increase in Brillouin shift. In Fig 3.1B, the sample size is increased, and the linear trend remains. At this stage, the large error bars are not indicative of lack of sensitivity in Brillouin imaging, but instead, that the gel manufacturing stage produces highly variable gels, as is not uncommon for radical polymer reactions. Variability in the gels that result from manufacturing is harmless: because this is a match-based comparative study, the 'true' stiffness is based off the measurements made by the DMA, not the formula used to make the gels, and Brillouin shift will be analyzed based on how well it 'follows' the DMA modulus readings. Sample variability in this way

would improve data quality by increasing the range of stiffnesses represented by the samples.

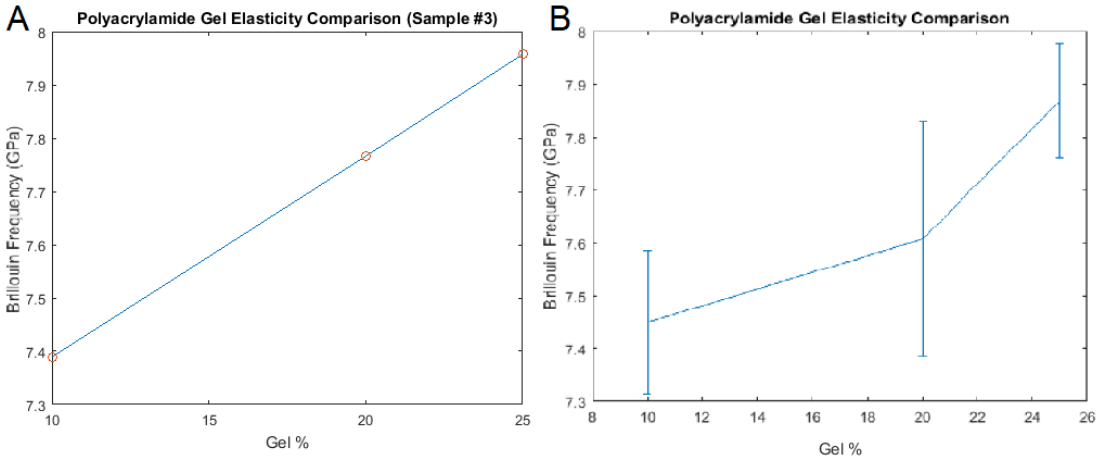

Fig 3.1: Analysis of the correlation of polyacrylamide concentration to detected Brillouin shift. (A): *N*=1, (B): *N*=5

On a preliminary basis, it appears a surface-level correlation has been successfully replicated between polyacrylamide polymer content (and thereby its elastic modulus) and the respective Brillouin shift, as supported by Fig. 3.2: X-axial total water content (which is the inverse of total polymer content/concentration) has a similar negative semi-linear correlation to both Young's modulus and longitudinal modulus. There does however appear to be a slight nonlinear relationship between water and longitudinal modulus, which may hint at a confounding factor that influences longitudinal modulus and doesn't affect Young's modulus in the same way, such as some phononic behavior of water. A suggestable next step would be to investigate a permutation array of gels with similar mechanical properties, but different compositions of water content, and observe any effects that may manifest in longitudinal modulus trends without being observable in Young's modulus correlations.

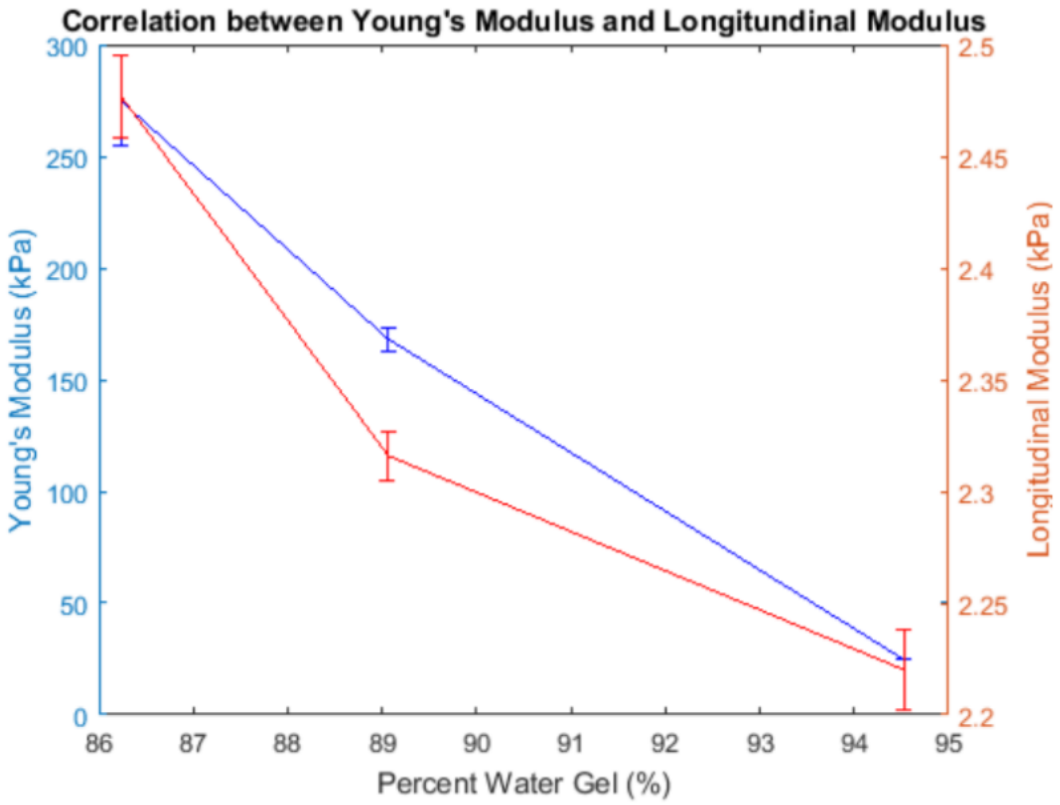

Fig. 3.2: A correlation plot between total water content (X-axis) and Young's Modulus (blue y-axis and line)/ and Longitudinal Modulus (orange y-axis and line) of 10%, 20%, and 25% polyacrylamide hydrogels.

3.3.2 States of water across permutation array

As a proof-of-concept for a permutation array, it was demonstrated that varying the composition of gel solely by its total polymer content can affect the presences of the various states of water described in 3.1.2 (Fig 3.2). Most notable differences can be observed between gels of approximately 10% original acrylamide concentration and gels of approximately 25% original acrylamide concentration. Even with by-sample variability, it is observable that free water and bound-freezing water make up dramatically less of the composition of concentrated polymer gels (compare ~60% bound water in 10_X samples to ~35% bound water in 25_X samples), and an even

more dramatic increase in nonfreezing-bound water between the two samples (compare ~5% in 10_X samples to ~30% in 25_X samples).

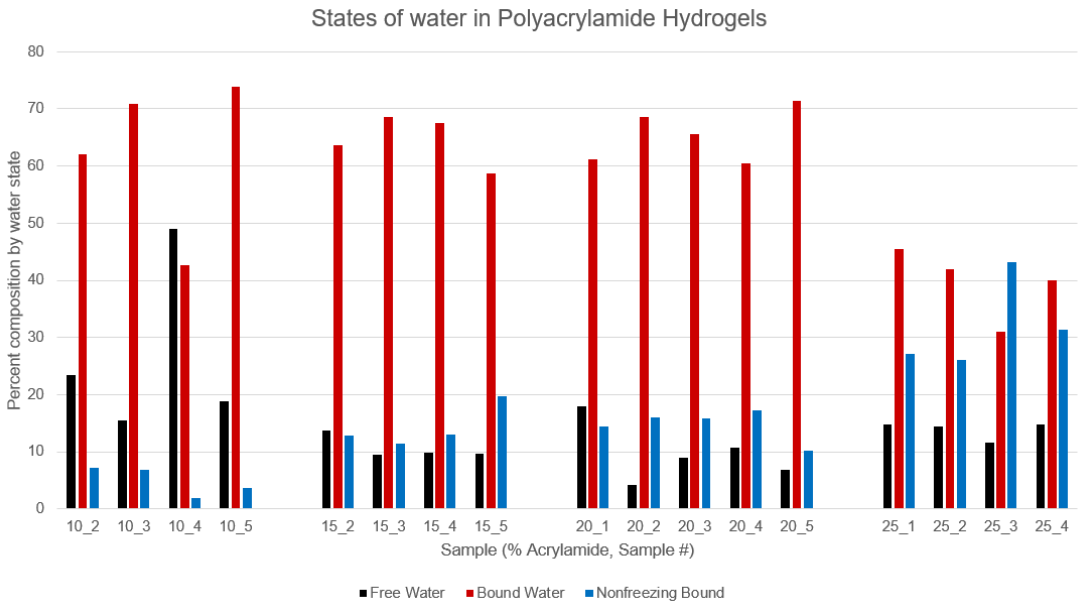

Fig 3.3: Comparison of the states of FF, BF, and BnF water across varying polyacrylamide concentrations.

An important distinction to draw, however is that each concentration group of these gels had dramatically different mechanical properties from each other group, meaning that any changes in longitudinal modulus as a result of the states of water could be masked by physical changes in mechanical properties instead. Though this demonstrates variability in states of water as a result of gel composition, to gain more insight into the factors influencing Brillouin shift, I reiterate that the next step should aim to create gels with similar mechanical properties that will unmask any effects of mechanical differences and allow for the relationship between water states and longitudinal modulus readings to be correlated. This could potentially be achieved by varying gel manufacturing parameters such as % crosslinking (3.2.1).

Bibliography

1. Church, D., Elsayed, S., Reid, O., Winston, B. & Lindsay, R. Burn wound infections. *Clin. Microbiol. Rev.* **19,** 403–434 (2006).
2. Kang, D.-K. *et al.* Rapid detection of single bacteria in unprocessed blood using Integrated Comprehensive Droplet Digital Detection. *Nat. Commun.* **5,** 5427 (2014).
3. Leibovici, L. *et al.* The benefit of appropriate empirical antibiotic treatment in patients with bloodstream infection. *J. Intern. Med.* **244,** 379–386 (1998).
4. Gao, F., Melody, T., Daniels, D. F., Giles, S. & Fox, S. The impact of compliance with 6-hour and 24-hour sepsis bundles on hospital mortality in patients with severe sepsis: a prospective observational study. *Crit. Care* **9,** R764-70 (2005).
5. Jordan, J. A. & Durso, M. B. Real-Time Polymerase Chain Reaction for Detecting Bacterial DNA Directly from Blood of Neonates Being Evaluated for Sepsis. *J. Mol. Diagnostics* **7,** 575–581 (2005).
6. Gao, W., Thamphiwatana, S., Angsantikul, P. & Zhang, L. Nanoparticle approaches against bacterial infections. *Wiley Interdiscip. Rev. Nanomedicine Nanobiotechnology* **6,** 532–547 (2014).
7. Surviving Sepsis Campaign. 3-Hour Bundle. *Surviv. Sepsis Campaign* (2012).
8. CDC. Antibiotic resistance threats in the United States, 2013. *Current* 114 (2013). doi:CS239559-B
9. Ventola, C. L. The antibiotic resistance crisis: part 1: causes and threats. *P T A peer-reviewed J. Formul. Manag.* **40,** 277–83 (2015).

10. WHO. Antimicrobial resistance. *Bull. World Health Organ.* **61,** 383–94 (2014).

11. Ibrahim, E. H., Sherman, G., Ward, S., Fraser, V. J. & Kollef, M. H. The Influence of Inadequate Antimicrobial Treatment of Bloodstream Infections on Patient Outcomes in the ICU Setting The Influence of Inadequate Antimicrobial Treatment of Bloodstream Infections on Patient Outcomes in the ICU Setting *. *CHEST J.* **118,** S146–S155 (2000).

12. Kim, J. S. *et al.* Antimicrobial effects of silver nanoparticles. **3,** 95–101 (2007).

13. Ayala-Núñez, N. V., Lara Villegas, H. H., Del Carmen Ixtepan Turrent, L. & Rodríguez Padilla, C. Silver nanoparticles toxicity and bactericidal effect against methicillin-resistant staphylococcus aureus: Nanoscale does matter. *Nanobiotechnology* **5,** 2–9 (2009).

14. Lara, H. H., Ayala-Núñez, N. V., Ixtepan Turrent, L. del C. & Rodríguez Padilla, C. Bactericidal effect of silver nanoparticles against multidrug-resistant bacteria. *World J. Microbiol. Biotechnol.* **26,** 615–621 (2010).

15. Rai, M., Yadav, A. & Gade, A. Silver nanoparticles as a new generation of antimicrobials. *Biotechnol. Adv.* **27,** 76–83 (2009).

16. Percival, S. L., Bowler, P. G. & Russell, D. Bacterial resistance to silver in wound care. *J. Hosp. Infect.* **60,** 1–7 (2005).

17. Morones-Ramirez, J. R., Winkler, J. A., Spina, C. S. & Collins, J. J. Silver Enhances Antibiotic Activity Against Gram-Negative Bacteria. *Sci. Transl. Med.* **5,** 190ra81-190ra81 (2013).

18. Cutting, K., White, R. & Hoekstra, H. Topical silver-impregnated dressings

and the importance of the dressing technology. *Int. Wound J.* **6,** 396–402 (2009).

19. Advanced Tissue. How to Remove Advanced Wound Care Products. (2016). Available at: https://www.advancedtissue.com/how-to-properly-remove-advanced-wound-care-products/. (Accessed: 30th March 2018)
20. Advanced Tissue. How To Remove Products When Changing Wound Dressings. (2014). Available at: https://www.advancedtissue.com/remove-wound-care-products-changing-dressings/. (Accessed: 30th March 2018)
21. Pickering, D. & Marsden, J. Techniques for aseptic dressing and procedures. *Community Eye Heal. J.* **28,** 17–17 (2015).
22. Behrens, A. M. *et al.* In Situ Deposition of PLGA Nano fi bers via Solution Blow Spinning. (2014).
23. Behrens, A. M. *et al.* Biodegradable-Polymer-Blend-Based Surgical Sealant with Body-Temperature-Mediated Adhesion. *Adv. Mater.* **27,** 8056–8061 (2015).
24. Feng, Q. L. *et al.* A mechanistic study of the antibacterial effect of silver ions on Escherichia coli and Staphylococcus aureus. (2000).
25. Morones, J. R. *et al.* The bactericidal effect of silver nanoparticles. *Nanotechnology* **16,** 2346–2353 (2005).
26. Leaper, P. D. Appropriate Use of Silver. *Wounds Int.* (2012).
27. Burd, A. *et al.* A comparative study of the cytotoxicity of silver-based dressings in monolayer cell, tissue explant, and animal models. *Wound Repair Regen.* **15,** 94–104 (2007).

28. Uygur, B., Craig, G., Mason, M. D. & Ng, A. K. Cytotoxicity and genotoxicity of silver nanomaterials. *Tech. Proc. 2009 NSTI Nanotechnol. Conf. Expo, NSTI-Nanotech 2009* **2,** 383–386 (2009).

29. Faust, R. A. Toxicity Summary for Silver. 1–8 (1992). doi:10.1016/B978-012673031-9/50018-6

30. Service, S. C. International Standard. *Communication* **2009,** 1–8 (2003).

31. Exudate Management. *Skilled MEDICAL* (2016). Available at: http://www.vicburns.org.au/minor-burns/minimise-infection/exudate-management/. (Accessed: 30th March 2018)

32. Wakshlak, R. B., Pedahzur, R. & Avnir, D. Antibacterial activity of silver-killed bacteria : the ‘ zombies ’ effect. *Sci. Rep.* 1–5 (2015). doi:10.1038/srep09555

33. Scarcelli, G. & Yun, S. H. Confocal Brillouin microscopy for three-dimensional mechanical imaging. *Nat. Photonics* **2,** 39–43 (2007).

34. Scarcelli, G. *et al.* Noncontact three-dimensional mapping of intracellular hydromechanical properties by Brillouin microscopy. *Nat. Methods* **12,** 1132–1134 (2015).

35. Scarcelli, G., Pineda, R. & Yun, S. H. Brillouin optical microscopy for corneal biomechanics. *Investig. Ophthalmol. Vis. Sci.* **53,** 185–190 (2012).

36. Wu, P. *et al.* Brillouin microscopy , what is it really measuring ?

37. Liu, Y. & Huglin, M. B. Observations by DSC on Bound Water Structure in Some Physically Crosslinked Hydrogels. *Polym. Int.* **37,** 63–67 (1995).